2024

The Dual Boundary Complex of the Moduli Space of Cyclic Compactifications

Toby Anderson

The Dual Boundary Complex of the Moduli Space of Cyclic Compactifications

Toby Anderson

Dagan Karp, Advisor
Siddarth Kannan, Advisor

Department of Mathematics

May, 2024

Abstract

Moduli spaces provide a useful method for studying families of mathematical objects. We study certain moduli spaces of algebraic curves, which are generalizations of familiar lines and conics. This thesis focuses on the dual boundary complex, $\Delta^{(r,n)}$, of the moduli space of genus-zero cyclic curves. This complex is itself a moduli space of graphs and can be investigated with combinatorial methods. Remarkably, the combinatorics of this complex provides insight into the geometry and topology of the original moduli space. In this thesis, we investigate two topologically invariant properties of $\Delta^{(r,n)}$. We compute its Euler characteristic, and we provide a conjecture and multiple possible proof techniques for calculating its homotopy type. Finally, we briefly discuss additional questions that might provide interesting future investigation of this complex.

Contents

List of Figures

Acknowledgments

To my thesis advisors, Professor Dagan Karp and Dr. Siddarth Kannan, thank you so much for all your amazing guidance and support you've provided me this year on thesis, graduate school applications, and beyond. I've learned a lot from this project and had a lot of fun.

To the thesis organizers (Professor Jon Jacobsen, Melissa Hernandez-Alvarez, and DruAnn Thomas), thank you for helping thesis run smoothly this year! And to the other thesis students, especially Clay Adams and Jasper Bown, thank you for your support and feedback on my writing and presentations throughout the year. I enjoyed spending time in thesis class together and getting to learn more about your theses.

To Professor Jamie Haddock, thank you being such an amazing mentor and professor. I am super grateful that I have had the opportunity to work with you so much through research, classes, and academic advising.

To Dr. Denise Machin, I will forever be grateful for CCBDC and the opportunities it granted me. You're an amazing mentor and teacher and have really created something special with CCBDC. I'm so glad that I get to continue working with you going forward.

To all my friends here at the 5Cs, Lauren Henson, Lawrence Nelson, Camilo Morales, Julia Hsing, Luke Stemple, Connor Seto, Svetlana Altshuler, Felix Murphy, Ford Ashmun, and many more, thank you for all the fun times in class, during ballroom, game nights, and beyond. I hope we all stay in touch.

To Ryan, thank you for the countless memories, I can't wait for many more with you. Thank you for all the support and continued interest in my thesis work, even though I was never able to explain it very well. I love you so much.

And to my family, my mom, dad, sister, and Bigdaddy, I am so incredibly grateful for all the love and support you've shown me my whole life, for my academic ambitions, for my identity, for everything. You all truly are the best family I could ask for. I love you all very much.

To everyone I listed above, I love you all and I couldn't have gotten to where I am today without you. I could write so much more, but I already had to make the text smaller so this fits on one page. This thesis is for all of you. Thank you ♡

Chapter 1

Introduction

When studying some mathematical object, rather than just focusing one one specific instance of that object, it may be more useful to study *all* objects of that type and learn how they behave as a family. For example, given a linear map $F : \mathbb{R}^m \to \mathbb{R}^n$, we may want to learn which points get mapped to $\vec{0}$. Rather than just one point, we often group all such points into the subset of the domain known as the *null space* or *kernel*. This type of reasoning motivates the idea of a *moduli space*.

Definition 1.1 (**Informal**). *A moduli space is a geometric space whose points represent isomorphism classes of algebraic or geometric objects.*

In other words, moduli spaces provide a concise way to describe unique instances of some class of mathematical objects. To gain some intuition, consider the following example of a moduli space.

Example 1.1. *Consider the moduli space of circles in $\mathbb{R}^2$ centered at the origin, where we consider two circles to be equivalent if they have the equal radii. A circle with radius r is given by the equation*

$$C_r : x^2 + y^2 = r^2$$

where $r > 0$. Thus, the moduli space of these circles is the positive real numbers, $\mathbb{R}^+$, where each $r \in \mathbb{R}^2$ represents the circle with radius r. We can extend this to circles in $\mathbb{R}^2$ centered at any point. At first, it might seem more difficult to find this moduli space since these circles are harder to compare than the subset of those centered at the origin. Note, however, that translating the circles does not affect their radii, and therefore does not change which ones we consider to be equivalent. By translating each circle to be centered at the origin, we can apply the same process

described previously. Thus, the moduli space of all circles in $\mathbb{R}^2$ *is* $\mathbb{R}^+$. (*See Figure* 1.1)

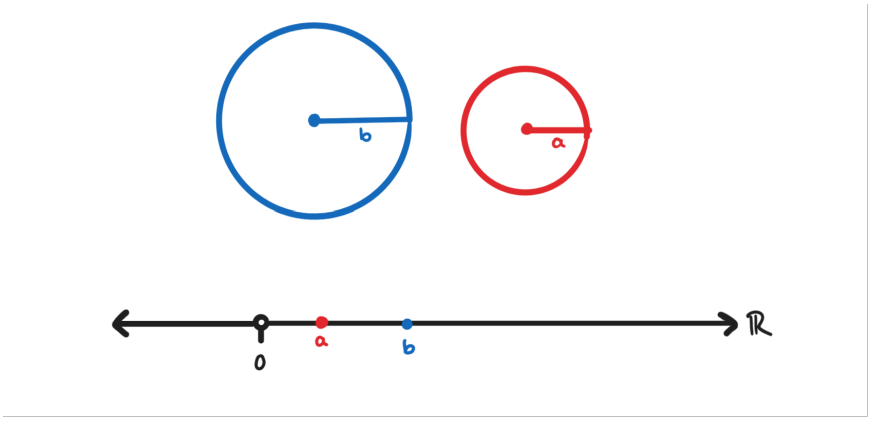

Figure 1.1 Two circles and their representative points in $\mathbb{R}^+$.

Example 1.2 (Brandt)**.** *For a slightly more complex example, consider the moduli space of triangles in* $\mathbb{R}^2$*, where we consider similar triangles to be equivalent* (*i.e. two triangles are equivalent if they only differ by scaling and rotating. Equivalent triangles have the same angles and ratios of side lengths*)*. To compare and these triangles in a way that doesn't change which ones we consider to be equivalent, rotate, scale, and translate each triangle so its shortest side is the line segment from* $(0,0)$ *to* $(0,1)$*. Then, a triangle is formed by choosing some point* (x,y) *as the third vertex. Does this mean the moduli space of triangles is* $\mathbb{R}^2$*? Sadly, it is not quite that simple. Because we want a unique point in our moduli space to represent classes of equivalent triangles, there are a few redundancies we need to consider.*

(1) *If the third vertex is located on the* y*-axis, we end up with a straight line, not a triangle. Thus,* $x = 0$ *is not in this moduli space.*

(2) *Triangles with third vertex* $(-x,y)$ *and* (x,y) *are similar since they only differ by a reflection across the* $y-$*axis. Thus, we only consider points where* $x > 0$ *in this moduli space.*

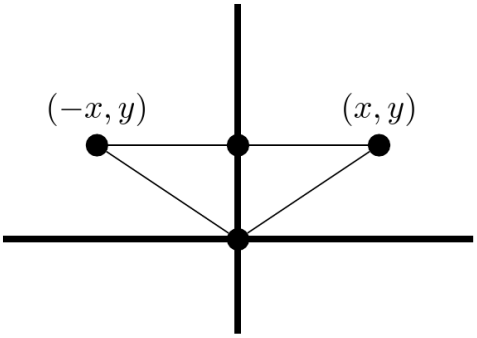

(3) *Similarly, triangles with the third point* (x, y) *and* $(x, -(y-1))$ *are equivalent, since they only differ by a reflection across* $y = 0.5$*, the midpoint of the shortest side. Therefore, we only consider points where* $y \geq 0.5$ *in this moduli space.*

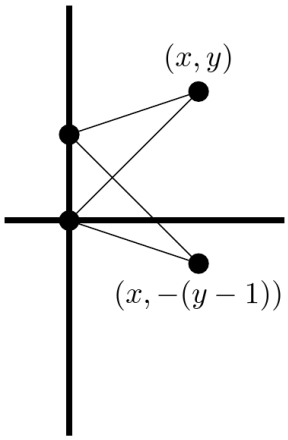

(4) *Finally, since we established the line segment* $(0, 0)$ *to* $(0, 1)$ *to be the shortest side of the triangle, we do not consider any points within Euclidean distance* 1 *of* $(0, 0)$ *or* $(0, 1)$*.*

Thus, the moduli space of triangles in $\mathbb{R}^2$ *can be visualized as the highlighted space shown in Figure* 1.2*.*

In algebraic geometry, a commonly studied moduli space is that of stable, n-pointed rational curves, $\mathcal{M}_{0,n}$, which we can visualize as n distinct marked points on a sphere. These curves and this moduli space will be described in more detail in Chapter 2. We consider two of these spheres to be equivalent

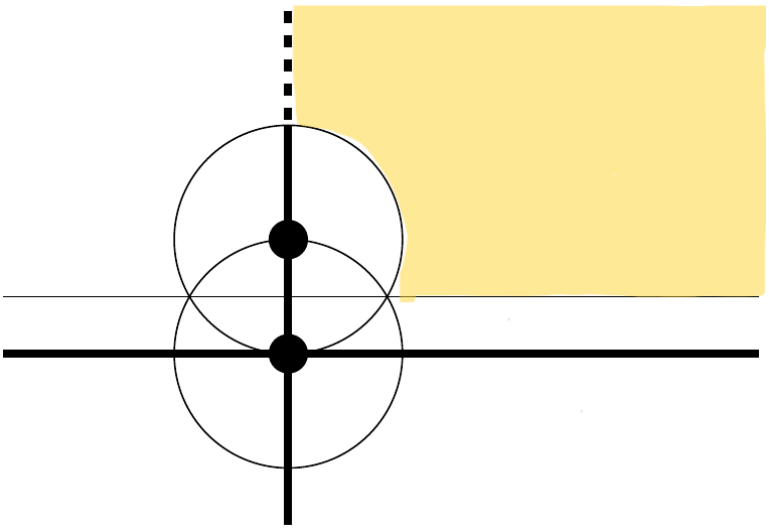

Figure 1.2 The moduli space of triangles in $\mathbb{R}^2$.

if there exists an automorphism that maps the marked points from one sphere to that of the other. An *automorphism* is an invertible function that maps a mathematical object to itself. Automorphisms of a sphere are Möbuis transformations (see Chapter 2 for the definition of a Möbius transformation). A curve in $\mathcal{M}_{0,n}$ is considered to be stable when it has only finitely many automorphisms. Notice that this is not true when it has two or fewer marked points (i.e. $n \leq 2$). By situating these points at the same point or two diametrically opposed points on the sphere, any rotation in which those points are the poles is an automorphism (of which there are infinitely many). Thus, only when $n \geq 3$ do we consider $\mathcal{M}_{0,n}$ to be stable.

Now, consider a situation in which two marked points try to coincide. Because we defined the marked points to be distinct, any sequence of points approaching each other will not have a limit. This underlies the fact that $\mathcal{M}_{0,n}$ is not a compact space. Compactness is a desirable feature of topological spaces as it guarantees many properties that make the space easier to work with. Thus, mathematicians have been motivated throughout the years to discover various ways to compactify $\mathcal{M}_{0,n}$.

This thesis studies one such compactification, $\overline{\mathcal{L}}_n^r$, which is a generalization of Losev-Manin space and was recently defined by Clader et al. (2022). Points in $\overline{\mathcal{L}}_n^r$ represent pointed cyclic curves satisfying a number of conditions, which will be explored in Chapter 2. Equivalently, $\overline{\mathcal{L}}_n^r$ parameterizes

the dual graphs of these curves, which lend themselves to combinatorial exploration. We can visualize the whole space of dual graphs with $\Delta^{(r,n)}$, the dual boundary complex of $\overline{\mathcal{L}}_n^r$. This can be thought of as a geometric realization of the set of dual graphs, and presents itself as an simplicial complex. A *simplicial complex* is a space built from *simplices*, which are n-dimensional generalizations of triangles. For example, a 0-dimensional simplex is a point, a 1-dimensional simplex is a line, a 2-dimensional simplex is a triangle, a 3-dimensional simplex is a tetrahedron, etc. An n-dimensional simplex is constructed from simplices that are degree n and below; Δ_n^r is an $(n-1)$-dimensional simplicial complex.

In this thesis, we use combinatorial methods to explore a variety of geometric and topological properties of Δ_n^r, notably, its Euler characteristic and homotopy type.

The Euler characteristic, denoted χ, was originally defined for surfaces of polyhedra according to the formula $\chi = V - E + F$, where V, E, and F represent the number of vertices, edges, and faces of the given polyhedron respectively. It is additionally a commonly used formula to identify planar graphs. In general, the Euler characteristic is a topological invariant and can be applied to simplicial complexes as follows.

Definition 1.2. *Let X be a simplicial complex and let $X[k]$ be the set of k-dimensional simplices in X. Then, the Euler characteristic, χ of X is defined as*

$$\chi(X) = \sum_{k=0}^{dim(X)} (-1)^k |X[k]|$$

In other words, it is the alternating sum of the number of m-dimensional simplices in X for all $m = 0, 1, \ldots, dim(X)$.

Homotopy type is a property of a topological space that provides insight into its general structure. If two spaces have the same homotopy type, we should be able to continuously deform one space to the other by compressing, dilating, and translating its parts, but without cutting, gluing, or ripping its parts. For example, we can continuously map $\mathbb{R}^2 \setminus \{(0,0)\}$ to a unit circle by sending each $x \in \mathbb{R}^2\{(0,0)\}$ to the nearest point on the circle (see Figure 1.3).

Thus, $\mathbb{R}^2 \setminus \{(0,0)\}$ and the unit circle have the same homotopy type. What if we did include the origin and instead tried to deform $\mathbb{R}^2$ to to unit circle? Notice that a unit circle has one hole while $\mathbb{R}^2$ does not. There is no way to continuously deform $\mathbb{R}^2$ to a circle without "ripping" it somewhere to

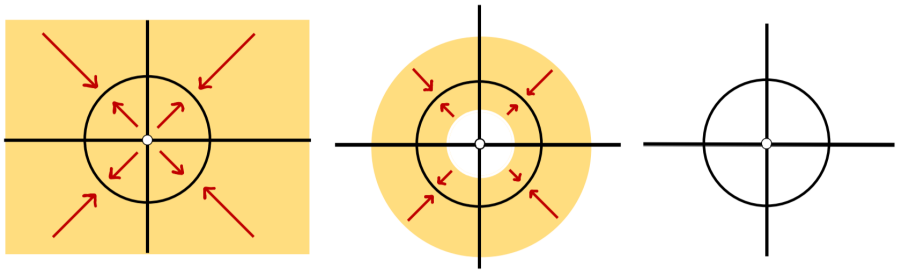

Figure 1.3 A continuous deformation from $\mathbb{R}^2 \setminus \{(0,0)\}$ to S^1.

create that hole. Thus, $\mathbb{R}^2$ and the unit circle do not have the same homotopy type.

In Chapter 2, this thesis will start by giving additional background on moduli spaces, specifically moduli spaces of stable marked curves, then, in Chapter 3, explain how we can use various combinatorial and graph theoretical representations to describe the boundary of these spaces. Chapter 4 provides example calculations of the dual graphs and $\Delta^{(r,n)}$ for small r, n. In Chapter 5, we delve into the investigation of the Euler characteristic of $\Delta^{(r,n)}$. We provide and prove that conjecture that $\chi(\Delta^{(r,n)} = 1 - (1-r)^n$. Chapter 6 details the homotopy type of $\Delta^{(r,n)}$. Although we do not prove its homotopy type, we provide a conjecture and discuss two possible proof techniques. We conclude with Chapter 7, which discusses future work for calculating the homotopy type, as well as other interesting questions about $\Delta^{(r,n)}$ that could be explored.

Chapter 2

Moduli Spaces of Stable Marked Curves

In this chapter, we take what we learned about moduli spaces in the previous chapter and introduce a few examples relevant to this thesis. We start by formulating projective space as a moduli space, then

we will introduce the concept of a moduli space, then provide examples of moduli spaces of stable, marked curves that build to the space studied in this thesis, $\overline{\mathcal{L}}_n^r$, which is the generalization of the Losev-Manin space.

2.1 $\mathbb{P}^1$ as a Moduli Space

Consider two distinct lines in the real, Euclidean plane. At how many points do they intersect? This depends, because if the lines are not parallel, they intersect at one point, but if they are parallel, they do not appear to intersect. By Bézout's theorem, for two curves C_1 and C_2 of degree m and n respectively, we expect mn intersection points (counting multiplicity). However, some might appear missing because they coincide, are complex, or, as in the case of the two parallel lines, occur at infinity.

Curves intersecting at infinity might sound unintuitive or impossible at first in the geometries we commonly work with. Thus, these examples motivate *projective geometries*, in which points at infinity are considered "normal" points and are handled in a uniform way. For example, consider the *complex projective line*, or $\mathbb{P}^1_{\mathbb{C}}$ (from now on, we omit the $\mathbb{C}$ when referring to this space). The complex projective line extends the complex numbers by adding a point at infinity. Essentially, $\mathbb{P}^1 = \mathbb{C}^1 \cup \{\infty\}$.

Definition 2.1. $\mathbb{P}^1$ *is defined as a moduli space of lines in* $\mathbb{C}^2$ *through the origin. Then,*

$$\mathbb{P}^1 = \{(x : y) \in \mathbb{C}^2 \mid (x : y) \neq (0 : 0)\}/\sim$$

where where $(x : y) \sim (\lambda x : \lambda y)$ *for any* $\lambda \neq 0$ *in* $\mathbb{C}$.

To understand $\mathbb{P}^1$, consider the geometry of the subset $U \subset \mathbb{P}^1$ such that $x \neq 0$. Then, there exists a bijection f from U to $\mathbb{C}$,

$$\begin{aligned} f : U &\to \mathbb{C} \\ (x : y) &\mapsto y/x. \end{aligned}$$

We see that f adheres to the equivalence relation, as $f((\lambda x : \lambda y)) = \lambda y/\lambda x = y/x$. This bijection has inverse

$$\begin{aligned} f^{-1} : \mathbb{C} &\to U \\ z &\mapsto (1 : z). \end{aligned}$$

Now, consider $\mathbb{P}^1 \setminus U$. Since $x = 0$, these ordered pairs have the form $(0 : y)$. Scaling by $1/y$, we see that this subset is equivalent to just one point $(0 : 1) \mapsto 1/0$.

Taking the union of these two subsets, we see that $\mathbb{P}^1 = \mathbb{C} \cup (0 : 1)$. Topologically, the complex plane is equivalent to $\mathbb{R}^2$, so how do we visualize $\mathbb{R}^2$ plus a point?

Definition 2.2 (Weisstein)**.** *The stereographic projection is a bijective map obtained by projecting points* P *on an* n*-dimentional sphere,* S^n*, from its north pole,* N*, to an* n*-dimensional plane,* $\mathbb{R}^n$*, tangent to its south pole with*

$$S^n \setminus \{N\} \longleftrightarrow \mathbb{R}^n$$

$$(x_1, \ldots, x_{n+1}) \longmapsto \left(\frac{x_1}{1 - x_{n+1}}, \ldots, \frac{x_n}{1 - x_{n+1}}\right)$$

$$\left(\frac{2y_1}{(\sum y_i^2) + 1}, \ldots, \frac{2y_n}{(\sum y_i^2) + 1}, \frac{(\sum y_i^2) - 1}{(\sum y_i^2) + 1}\right) \longmapsto (y_1, \ldots, y_n).$$

See figure 2.1 *for a visualization.*

Under the stereographic projection, every point on S^2 except N is mapped to a point on $\mathbb{R}^2$, so $\mathbb{R}^2$ is topologically equivalent to a sphere minus a point. Applying this to $\mathbb{P}^1$, we note that the subset U is topologically equivalent to S^2 minus a point, N. However, $\mathbb{P}^1$ has the additional point $(0 : 1)$, so we

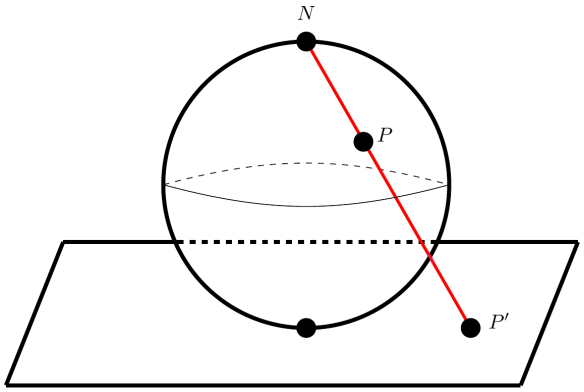

Figure 2.1 The stereographic projection from S^2 to $\mathbb{R}^2$.

can define this point as mapping to and from N. Thus, $\mathbb{P}^1$ is topologically equivalent to the S^2, and will be visualized as such for the in this thesis. Additionally, we consider the point $(0:1)$ to be the point at infinity. To see why, note that trying to project $N = (0:1)$ to $\mathbb{R}^2$ using the stereographic projection, we get a line that runs parallel to the plane. In other words, we could say that $(0:1)$ projects to$\mathbb{R}^2$ at infinity.

2.2 Moduli Space of n Points on $\mathbb{P}^1$

$\mathcal{M}_{0,n}$ is the moduli space of n-marked smooth curves of genus zero up to some isomorphism class. Equivalently, $\mathcal{M}_{0,n}$ is a moduli space of isomorphism classes of n ordered distinct marked points on $\mathbb{P}^1$. Formally,

$$\mathcal{M}_{0,n} = \{(p_1, p_2, \ldots, p_n) \in \mathbb{P}^1 \mid p_i \neq p_j \text{ for } i \neq j\},$$

under an equivalence relation, $\sim$, such that consider $(p_1, p_2, \ldots, p_n) \sim (q_1, q_2, \ldots, q_n)$ if and only if there exists some automorphism of $\mathbb{P}^1$, Φ, such that $\Phi(p_i) = q_i$ for all i. We denote the set of all automorphisms of $\mathbb{P}^1$ as $\mathrm{Aut}(\mathbb{P}^1)$. In general, automorphisms of $\mathbb{P}^1$ are Möbius transformations.

Definition 2.3. *Möbius transformations are rational functions from $\mathbb{P}^1$ to $\mathbb{P}^1$ of the form*

$$z \to \frac{az + b}{cz + d},$$

where $a, b, c, d, z \in \mathbb{C}$ and $ad - bc \neq 0$. Geometrically, Möbius transformations first apply the inverse stereographic projection from $\mathbb{P}^1$ to S^2, moving and rotating

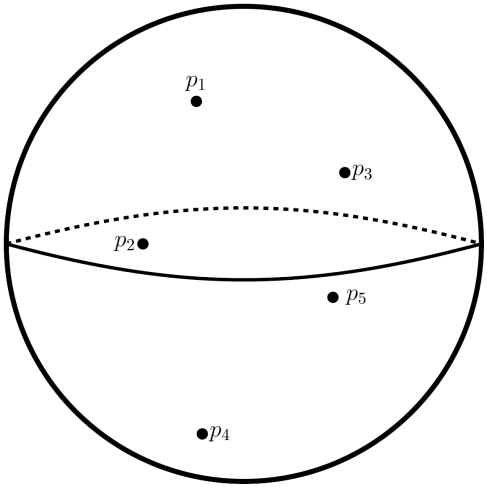

Figure 2.2 Visualization of a point in $\mathcal{M}_{0,5}$

the sphere to a new orientation, then applying the stereographic projection to get back to $\mathbb{P}^1$.

We can also think of automorphisms of $\mathbb{P}^1$ as a part of the projective linear group $PLG_2(\mathbb{C})$.

Definition 2.4. *The projective linear group* $PLG_2(\mathbb{C})$ *consists of* 2×2 *invertible matrices with nonzero determinant under an equivalence relation such that transformations scaled by some* $\lambda \in \mathbb{C}^*$ *are isomorphic. In other words,*

$$\begin{pmatrix} a & b \\ c & d \end{pmatrix} \sim \begin{pmatrix} \lambda a & \lambda b \\ \lambda c & \lambda d \end{pmatrix}$$

where $a, b, c, d \in \mathbb{C}$. *Then, a point* $(x : y) \in \mathbb{P}^1$ *is transformed to* $(ax + by : cx + dy)$.

An element $\Phi \in \mathrm{Aut}(\mathbb{P}^1)$ is uniquely determined by its action on three distinct points. In other words, for $p_1, p_2, p_3 \in \mathbb{P}^1$ and $\Phi, \Phi' \in \mathrm{Aut}(\mathbb{P}^1)$, if $\Phi(p_1) = \Phi'(p_1)$, $\Phi(p_2) = \Phi'(p_2)$, and $\Phi(p_3) = \Phi'(p_3)$, then $\Phi = \Phi'$. Additionally, for some $q_1, q_2, q_3 \in \mathbb{P}^1$, there exists a unique $\Phi \in \mathrm{Aut}(\mathbb{P}^1)$ such that $\Phi(p_1) = q_1$, $\Phi(p_2) = q_2$, and $\Phi(p_3) = q_3$. Thus, we can see that $\mathcal{M}_{0,3}$, for example, is a single point. This point is typically delineated $\{(0, 1, \infty)\}$. As a further example, we can see that

$$\mathcal{M}_{0,4} = \mathbb{P}^1 \setminus \{0, 1, \infty\}.$$

In other words, given four points $(p_1, p_2, p_3, p_4) \in \mathbb{P}^1$, we can always perform the unique automorphism of sending (p_1, p_2, p_3) to $(1, 0, \infty)$. Then, the isomorphism class is determined by where p_4 is sent. Note that p_4 cannot be sent to $0, 1$, or ∞, as we defined $p_i \neq p_j$ when $i \neq j$. Going a step father, a point in $\mathcal{M}_{0,5}$ has equivalence class Representative

$$(0, 1, \infty, \Phi(p_4), \Phi(p_5)),$$

where $\Phi \in \mathrm{Aut}(\mathbb{P}^1)$. Thus,

$$\mathcal{M}_{0,5} = (\mathcal{M}_{0,4} \times \mathcal{M}_{0,4}) \setminus \{\text{diagonal}\},$$

where the diagonal refers to points in which $\Phi(p_4) = \Phi(p_5)$. In general,

$$\mathcal{M}_{0,n} = (\overbrace{\mathcal{M}_{0,4} \times \cdots \times \mathcal{M}_{0,4}}^{n-3 \text{ times}}) \setminus \{\text{all diagonals}\}.$$

As an additional way to formulate $\mathcal{M}_{0,n}$, we can turn to configuration spaces.

Definition 2.5. *For a topological space X, the configuration space $Conf_n(X)$ is the set of ordered n-tuples of distinct points on X.*

We can alternatively define $\mathcal{M}_{0,n}$ as the quotient space $\mathrm{Conf}_n(\mathbb{P}^1)/\sim$, where $(p_1, p_2, \ldots, p_n) \sim (q_1, q_2, \ldots, q_n)$ if and only if there exists an automorphism Φ of $\mathbb{P}^1$ such that $(\Phi(p_1), \Phi(p_2), \ldots, \Phi(p_n)) = (q_1, q_2, \ldots, q_n)$. In general,

$$\mathcal{M}_{0,n} \cong \mathrm{Conf}_{n-3}(\mathbb{P}^1 \setminus \{0, 1, \infty\})$$

for $n \geq 4$.

2.3 Compactifications of $\mathcal{M}_{0,n}$

For all $n \geq 4$, $\mathcal{M}_{0,n}$ is not compact. Notably, there are missing "limit points;" for example, $\mathcal{M}_{0,4}$ is missing the points 0, 1, and ∞. Importantly, points are not allowed to coincide. Therefore, any sequence in which a point is approaching a missing point or two points are approaching each other does not have a limit.

There are many reasons that compactness is a desirable quality for moduli spaces; as an example, compact spaces are better suited for intersection theory, which then allows for their use in enumerative geometry (Cavalieri, 2016). Thus, several compactifications of $\mathcal{M}_{0,n}$ have been proposed over the years.

2.3.1 $\overline{\mathcal{M}}_{0,n}$

Discovered by Deligne and Mumford (1969), one way to compactify $\mathcal{M}_{0,n}$ is to allow points that are trying to coincide to "bubble off" onto a new component (i.e. a new copy of $\mathbb{P}^1$). When this occurs, the resulting curves are called *degenerations*. The point at which components in these degenerations meet is called a *double point*. This provides us with the space $\overline{\mathcal{M}}_{0,n}$. More formally, we can define $\overline{\mathcal{M}}_{0,n}$ as the moduli space of stable rational n-pointed curves.

Definition 2.6. *Cavalieri A stable rational n-pointed curve is a tuple* $(C, p_1, \ldots, p_n)$ *such that*

(1) *C is a connected curve of genus* 0 *whose only singularities are double points,*

(2) $(p_1, \ldots, p_n)$ *are distinct points of C and are not located at the singularities, and*

(3) *the only automorphism of C that preserves the marked points is the trivial automorphism.*

Condition (3) of Definition 2.6 requires that, in order for a curve in $\overline{\mathcal{M}}_{0,n}$ to be stable, each component must have at least three *special points*, where a special point is either a double point or one of the marked points.

Example 2.1. *Figure* 2.3 *pictures all unique degenerations in* $\overline{\mathcal{M}}_{0,4}$*. Any further degenerations are not stable* (*i.e. at least one component has fewer than three special points*).

Example 2.2. *Figure* 2.4 *shows degenerations in* $\overline{\mathcal{M}}_{0,5}$*. The figure is not exhaustive.*

2.3.2 Hasset Space

Hassett (2003) presented an alternate compactification of $\mathcal{M}_{0,n}$ that assigns weights to each of the marked points. This produces $\overline{\mathcal{M}}_{0,w}$, which is the moduli space of weighted stable rational curves.

Definition 2.7. *Let* $w \in \mathbb{Q}^n$ *be a weight vector with* $0 < w_i \leq 1$ *for all* $i = 1, 2, \ldots, n$*. A weighted stable rational curve is a tuple* $(C, p_1, \ldots, p_n)$ *such that*

(1) *C is a curve of genus* 0*,*

(2) $p_1, \ldots, p_n$ *are n smooth points of C and if two points* p_i *and* p_j *coincide,* $w_i + w_j < 1$*, and*

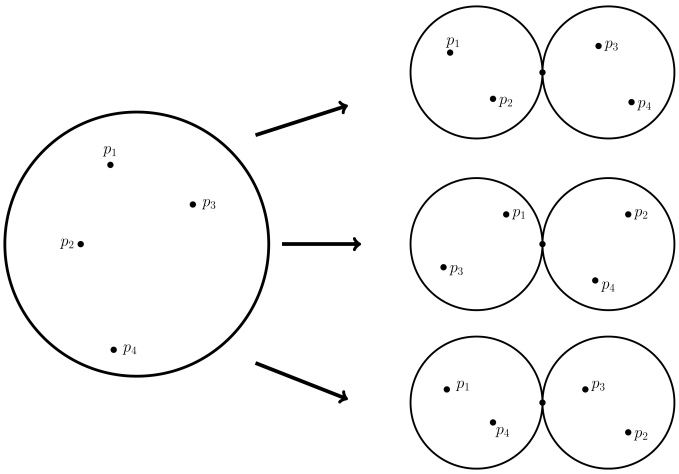

Figure 2.3 Stable degenerations in $\overline{\mathcal{M}}_{0,4}$.

(3) *on each component of C, the number of nodes plus the sum of the weights must be strictly greater than 2.*

2.3.3 Losev-Manin Space

The Losev-Manin space, $\overline{\mathcal{L}}_n$ was proposed by Losev and Manin (2000) as another compactification of $\mathcal{M}_{0,n}$. It generalizes Hasset spaces, which are recovered in the special case when the weight data $w = (1, 1, \epsilon, \epsilon, \ldots, \epsilon)$. The points with weight 1 are "heavy"—they are not allowed to coincide with other marked points—and the n points with weight ϵ are "light"—they are allowed to coincide with other light points.

2.3.4 Generalizations of Losev-Manin Space

Batyrev and Blume (2009) extended the work of Losev and Manin by constructing the moduli space $\overline{\mathcal{L}}_n^2$ with an involution σ, two fixed light points of σ, one heavy orbit of marked points, and n light marked points. Recently, Clader et al. (2022) generalized this to $\overline{\mathcal{L}}_n^r$.

Definition 2.8. *In $\mathbb{C}$, $z^r = 1$ has r solutions of the form $e^{2k\pi i/r}$ for $k \in \{0, 1, \ldots, r\}$. These are the rth roots of unity. They form a cyclic group of order r under multiplication, which is generated by $e^{2k\pi i/r}$ when $gcd(k, r) = 1$. These are called the primitive roots of unity.*

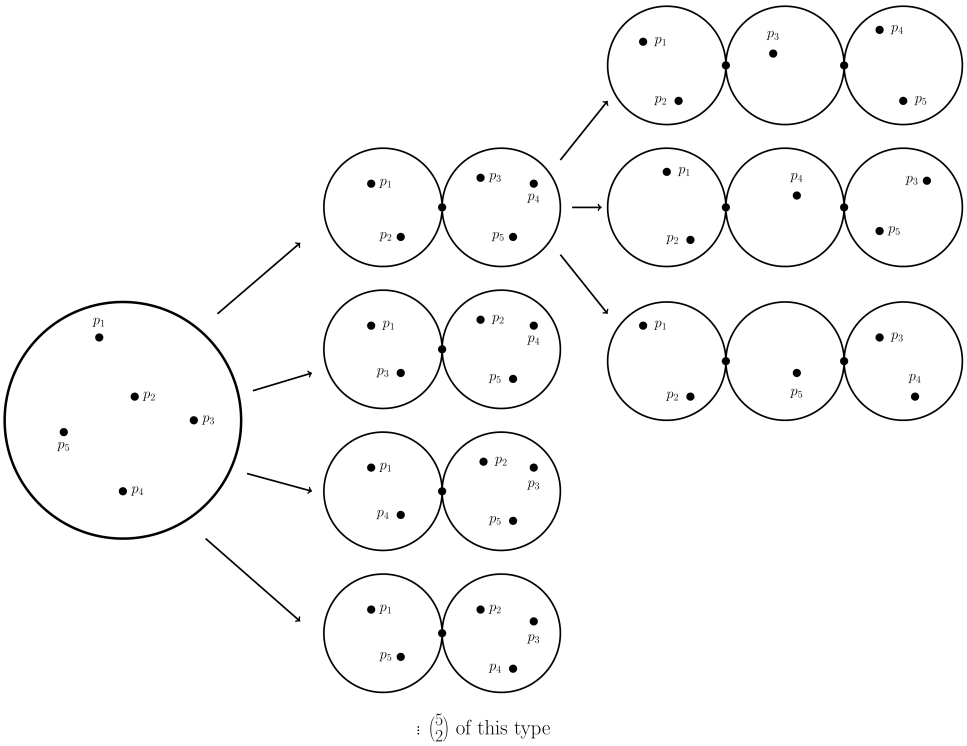

Figure 2.4 Stable degenerations in $\overline{\mathcal{M}}_{0,5}$.

The space $\mathcal{L}_n^r$ parameterizes n orbits of light marked points of points on $\mathbb{P}^1$ under the action by the r^{th} roots of unity, μ_r. There also exists an $(n+1)^{\text{th}}$ heavy orbit. The fixed points $\{0, \infty\}$ (often denoted $\{x^+, x^-\}$) may coincide with the light orbits, but must remain separate from the heavy orbit.

Using similar intuition as to that behind the fact that $\mathcal{M}_{0,n}$ isn't compact, we find that $\mathcal{L}_n^r$ is not compact as well. We note that a sequence of points trying to coincide with any point in the heavy orbit will not have a limit. Thus, the following compactification is presented.

Definition 2.9 (Clader et al.)**.** *An r-pinwheel curve is a tree of projective lines meeting at nodes, consisting of a central $\mathbb{P}^1$ from which r equal-length chains of $\mathbb{P}^1$s (called spokes) emanate. If the spokes have length k, we say that the pinwheel curve has length k (See figure 2.5).*

Definition 2.10 (Clader et al.)**.** *An (r, n)-curve consists of*

(1) *an r-pinwheel curve C,*

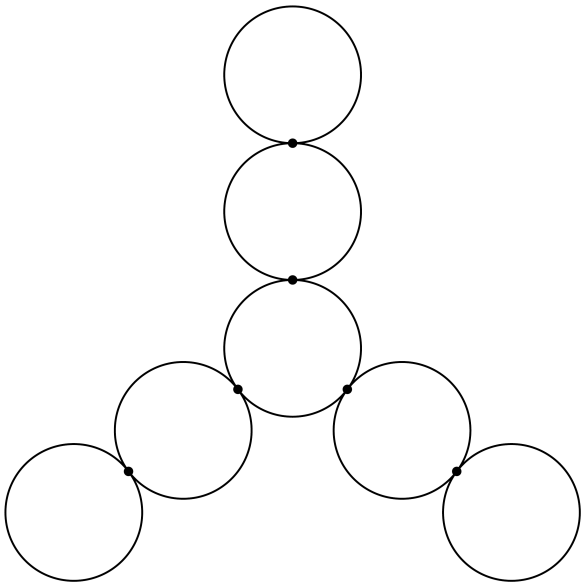

Figure 2.5 A 3-pinwheel curve of length two.

(2) *an automorphism $\sigma = C \longrightarrow C$ of order r rotation,*

(3) *two distinct fixed points x^+ and x^- of σ,*

(4) *n labeled orbits of σ, $(z_1^0, \ldots, z_1^{r-1}), \ldots, (z_n^0, \ldots, z_n^{r-1})$ such that $\sigma(z_i^j) = z_i^{j+1(mod r)}$, and*

(5) *an additional orbit $(y^0, \ldots, y^{r-1})$ such that $\sigma(y^l) = y^{l+1(mod r)}$ which are distinct from one another as well as from the z_i^j's and the fixed points.*

An (r, n)-curve is stable if each component of C contains at least two heavy points (nodes or y^l) and any components with exactly two heavy points must contain at least one of $x^\pm$ or z_i^j. This forces the requirement that

(1) $y^0, \ldots, y^{r-1}$ must lie on the r leaves of the pinwheel curve,

(2) the automorphism σ must be a rotation taking each spoke to another, and

(3) the fixed points $x^\pm$ must lie on the central component.

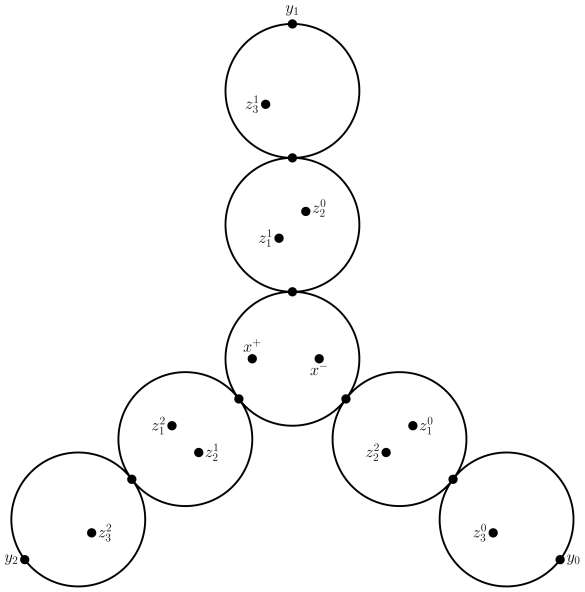

Figure 2.6 A stable (3,3)-curve.

Then, $\overline{\mathcal{L}}_n^r$, the compactification of $\mathcal{L}_n^r$, is the moduli space of stable (r, n)-curves.

Chapter 3

Combinatorics of the Boundary

In this chapter, we explore the ways in which the boundary of $\overline{\mathcal{M}}_{0,n}$ and $\overline{\mathcal{L}}_n^r$ can be defined combinatorically. We define the boundary of some space X as $\overline{X} \setminus X$, or in other words, the elements in the compactification that are not in the original space X. We will introduce dual graphs, then show how those can be used to construct the dual boundary complex for both $\overline{\mathcal{M}}_{0,n}$ and $\overline{\mathcal{L}}_n^r$.

3.1 Dual Graphs of $\overline{\mathcal{M}}_{0,n}$

Definition 3.1. *An n-marked tree is a connected finite tree T together with bijection*

$$\textit{leaves}(T) \longleftrightarrow \{1, \ldots, n\}$$

where leaves(T) refers to the set of vertices in T with degree 1.

We can represent points in the boundary of $\overline{\mathcal{M}}_{0,n}$ as *n-marked stable trees* in which

(1) each component and marked point is represented by a vertex,

(2) there is an edge between a marked point and the components in which it is contained, and

(3) there is an edge between components that share a double point Chan.

Thus, an n-marked tree being stable implies no vertices of degree two; each marked point corresponds to a leaf and each component should have

degree at least three. Any vertex with degree two implies a component with only two special points, which is not stable.

These n-marked stable trees give us the *dual graphs* of the boundary of $\overline{\mathcal{M}}_{0,n}$. The set of all these dual graphs is denoted $\Gamma_{0,n}$.

Example 3.1. *The boundary points of* $\overline{\mathcal{M}}_{0,4}$ *can be represented with the following* 4*-marked stable trees*:

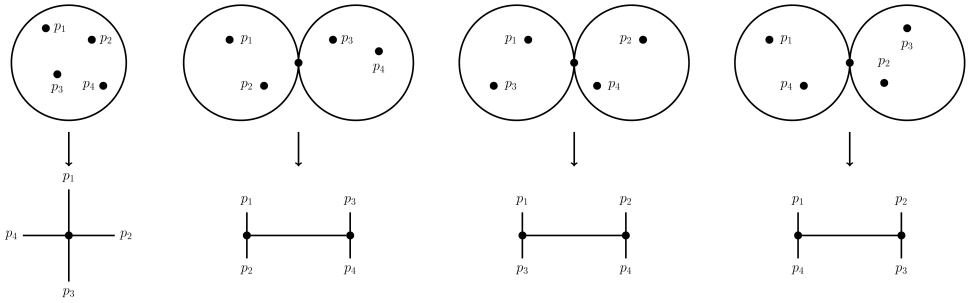

Example 3.2. *The following are examples of* 5*-marked stable trees for the boundary points of* $\overline{\mathcal{M}}_{0,5}$.

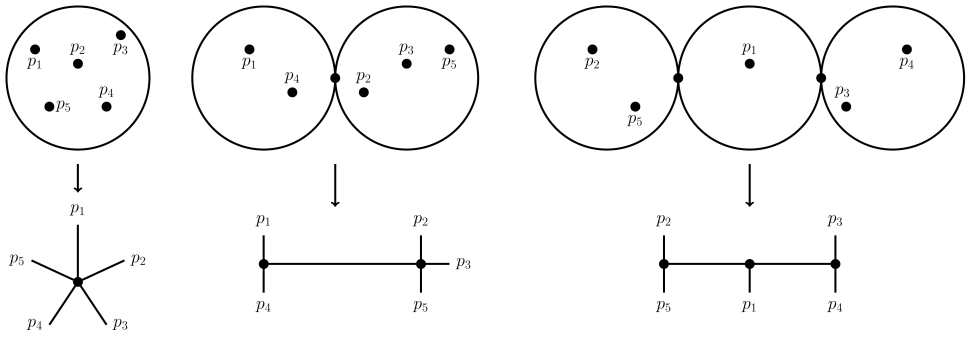

3.2 Dual Graphs of $\overline{\mathcal{L}}_n^r$

Similarly, we can define the boundary of $\overline{\mathcal{L}}_n^r$ using dual graphs as well. These graphs are (r, n)-trees, in which there are

(1) nodes for each component,

(2) edges between the connected components (i.e. components that share a node), and

(3) leaves for each point on an orbit and both fixed points.

The stability conditions for (r, n)-curves listed in the previous chapter induce stability conditions for (r, n)-trees. For an (r, n)-tree to be stable,

(1) no node can be of degree two (the marked and fixed points are leaves with degree one and the nodes representing components must have degree at least three),

(2) the heavy orbit $(y^0, \ldots, y^{r-1})$ must be incident to the outermost modes,

(3) the fixed points x^+, x^- must be incident to the central vertex, and

(4) there must be at least one light marked point z_i^j on each of the non-central nodes.

The *length* of a tree is the number of internal edges (i.e. edges between components) that emanate from the central component on each of the r spokes. The stability conditions imply that stable (r, n)-trees range in length from 1 to n.

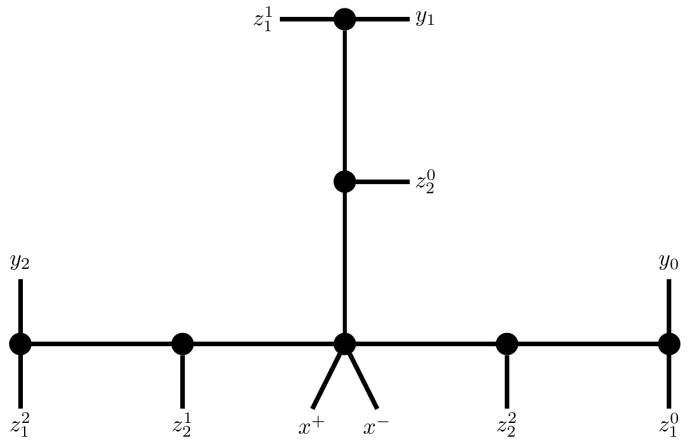

Figure 3.1 A stable (3,2)-tree of length two.

The set of all dual graphs of the boundary of $\overline{\mathcal{L}}_n^r$ is denoted $\Gamma^{(r,n)}$.

3.3 Dual Boundary Complex of $\overline{\mathcal{M}}_{0,n}$

There exists a bijection between boundary strata in $\overline{\mathcal{M}}_{0,n}$ and isomorphism classes of n-marked stable trees with at least one internal edge.

Let $\Delta_{0,n}$ be the topological space defined by

$$\Delta_{0,n} = \left\{ (T, l) \mid T \in \Gamma_{0,n},\ l : \text{Internal Edges}(T) \to \mathbb{R}_{\geq 0},\ \sum_{e \in \text{IE}(T)} l(e) = 1 \right\}.$$

In other words, $\Delta_{0,n}$ is the space of n-marked stable trees with at least one internal edge such that these internal edges are labeled with nonnegative real numbers that all sum to one.

Example 3.3. *Let T be the following tree in $\Gamma_{0,5}$:*

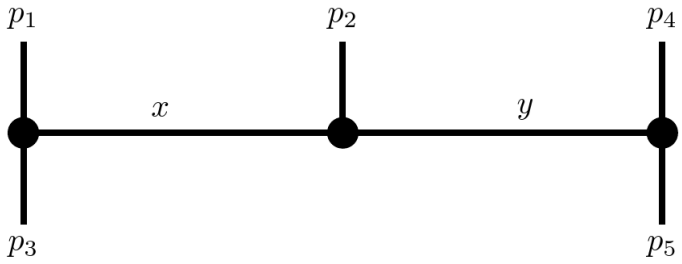

Then, we want to know the space of all length functions of the internal edges x and y such that $x + y = 1$. This space is given by

$$\{(x, y) \in \mathbb{R}^2 \mid x, y \geq 0,\ x + y = 1\}.$$

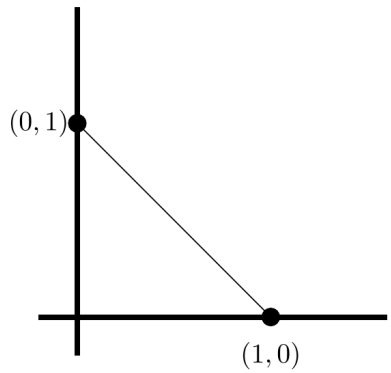

We can see that this space is a 1-simplex.

Definition 3.2. *A standard simplex is given by*

$$\sigma_n = \left\{ (x_1, \ldots, x_n) \mid x_i \geq 0, \sum_{x_i} = 1 \right\}.$$

We can think of simplices as generalizations of triangles. For example, a 0-simplex is a point, a 1-simplex is an line, a 2-simplex is a triangle, a 3-simplex is a tetrahedron, etc. The simplex defined by any subset of the $n+1$ points that define an n-simplex is a *face* of that simplex.

Definition 3.3. *A simplicial complex K is a topological space that is built from a set of simplices under the following conditions*:

1. *The faces of each simplex $\sigma \in K$ are also in K.*
2. *Any nonempty intersection of two simplices σ_1, σ_2 in K is a face of each.*

For example, a graph is a 1-dimensional simplicial complex.

In general, if $T \in \Gamma_{0,n}$ with $k+1$ internal edges, then the space $\sigma(T)$ of length functions on the internal edges of T of total length one is a standard k-simplex.

We can define $\Delta_{0,n}$ as

$$\Delta_{0,n} = \left(\bigsqcup_{T \in \Gamma_{0,n}} \sigma(T) \right) / \sim$$

where $\sim$ is the equivalence relation such that an internal edge that is labeled with a 0 is the same as that edge being contracted (Chan, 2017).

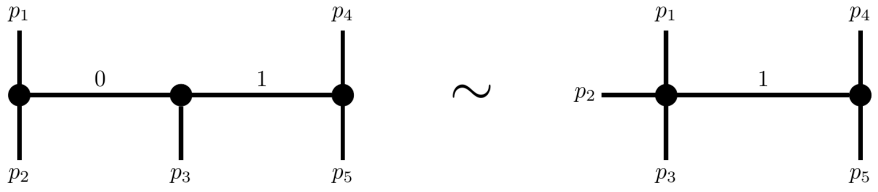

Figure 3.2 An example of two equivalent dual graphs

In general, $\Delta_{0,n}$ is an $(n-4)$-dimensional simplicial complex. We call $\Delta_{0,n}$ the *dual boundary complex* of $\overline{\mathcal{L}}_n^r$.

Example 3.4. *The dual boundary complex of* $\overline{\mathcal{M}}_{0,4}$, $\Delta_{0,4}$, *is a* 0*-dimensional simplicial complex consisting of three vertices. The vertices are labeled with the dual graphs they represent.*

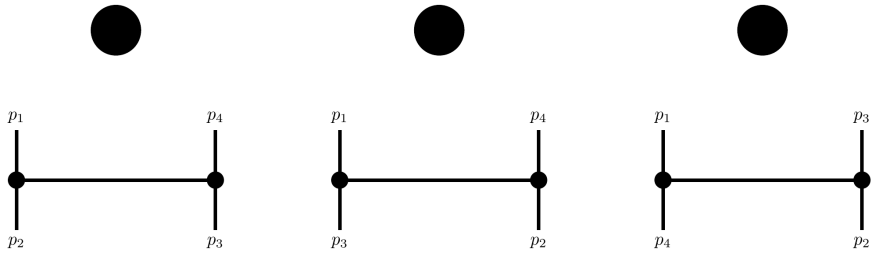

Example 3.5. *The dual boundary complex of* $\overline{\mathcal{M}}_{0,5}$ *is a* 1*-dimensional simplicial complex (i.e. a graph). A partial construction is shown below, where the vertices and edges are labeled with the dual graphs they represent.*

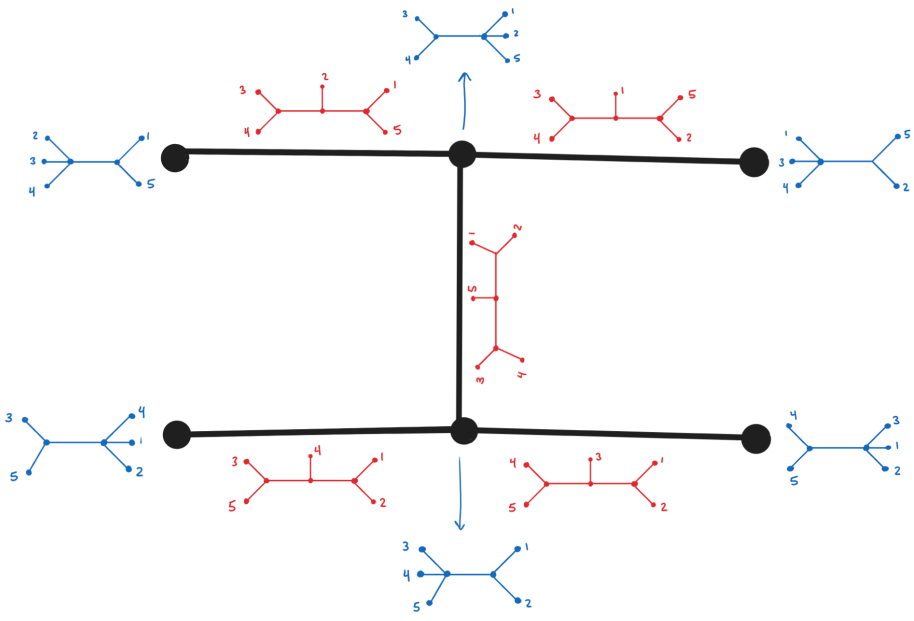

When completed, $\Delta_{0,5}$ is isomorphic to the Petersen graph.

3.4 Dual Boundary Complex of $\overline{\mathcal{L}}_n^r$

Similarly, we can define the dual boundary complex of $\overline{\mathcal{L}}_n^r$, which is the geometric realization of $\Gamma^{(r,n)}$.

Let $\Delta^{(r,n)}$ be the topological space defined by

$$\Delta^{(r,n)} = \{(G, l) \mid G \in \Gamma_n^r,\ l : \text{Internal Edges}(G) \to \mathbb{R}_{\geq 0}\}/\sim$$

Additionally, the metric function l must satisfy the following conditions:

(1) l is constant on orbits of edges, that is, l assigns the same value to edges in the same orbit, and

(2) the sum of the total metrics is fixed to r. Combined with the first condition, this forces the metrics of edges of each spoke to add to 1.

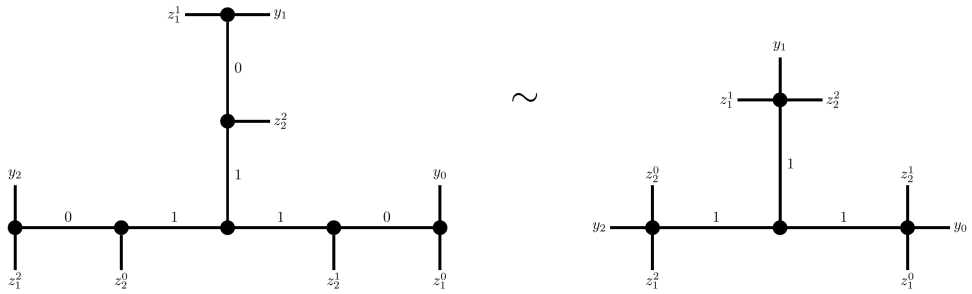

Figure 3.3 An example of two equivalent dual graphs with labeled edge lengths.

In general, Δ_n^r is a $(n-1)$-dimensional simplicial complex. Dual graphs corresponding to (r, n)-curves of length k are represented by $(k-1)$-dimensional simplices. These simplices are adjacent if there exists an (r, n)-stable tree such that contracting one orbit of edges produces an (r, n)-stable curve that is isomorphic to the other.

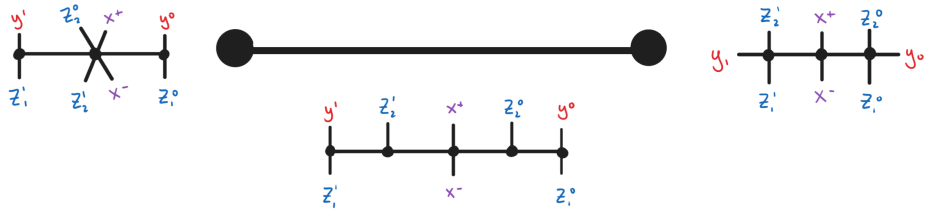

Figure 3.4 An example of how simplicies in $\Delta^{(2,2)}$ are connected by edge contractions of the dual graphs they represent.

Examples of $\Delta^{(r,n)}$ are presented in the next chapter.

Chapter 4

Example Calculations

In this chapter, we present calculations of $\Gamma^{(r,n)}$ and $\Delta^{(r,n)}$ for small r, n. We also present a proposition about the number of maximal trees in $\Gamma^{(r,n)}$. Note that in this chapter, we do not label the fixed points x^+ and x^- on the (r, n)-trees; they are the unlabeled leaves on the central component. Additionally, when calculating the number of trees of each length in sections 4.3, 4.4, and 4.5, we assume that the component to which each y^i is incident is fixed (see figure 4.1 for an example). Figures showing the result of all of these calculations are given in section 4.6.

4.1 When $n = 1$

With only one orbit of light marked points, all trees in $\Gamma^{(r,1)}$ are length one. Each tree is uniquely determined by the component on which z_1^0 is located (i.e. with which y^i it shares a node), as the automorphism σ will determine where the rest of the points in the orbit are sent. Thus, there are r trees of length 1 in $\Gamma^{(r,1)}$, and $\Delta^{(r,n)}$ consists of r 0-simplices.

4.2 Maximal trees in $\Gamma^{(r,n)}$

For any n, the longest a tree in $\Gamma^{(r,n)}$ is length n. Based on If the length k was larger than n, we would have n orbits for $k > n$ components on each spoke, so by the Pigeonhole principle, at least one component will not contain a light marked point. This goes against the stability conditions.

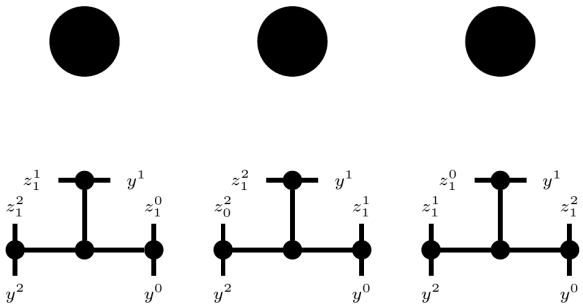

Figure 4.1 $\Delta^{(3,1)}$ consists of three vertices that correspond to length one trees.

The only way to create a stable tree of length n is with exactly one light orbit z_i^j on each non-central component.

Proposition 4.1. *There are $r^n \cdot n!$ trees of length n in $\Gamma^{(r,n)}$.*

Proof. There are $n!$ distinct ways to order the n orbits $(z_i^0, \ldots, z_i^{r-1})$ on the n components. Then, consider z_i^0 for each of the n orbits of points. There are r spokes on which to assign this point; the rest are determined by the involution σ. Thus, there are $r^n \cdot n!$ distinct trees of length n in $\Gamma^{(r,n)}$ as desired. □

4.3 Calculation of $\Gamma^{(2,2)}$ and $\Delta^{(2,2)}$

With two orbits of light marked points, trees in $\Gamma^{(2,2)}$ will be either length two or length one. There are two different options of what trees of length one could look like.

(1) We could assign both orbits of points to the outside components. Then, for both orbits, there are two choices for which point to assign to the same component as y^0. Thus, there are four of those length-one trees.

(2) Alternatively, we can assign one orbit of points to the central component and the other to outside components. In this case, there are two choices for which orbit to assign to the outside component, and another two choices for which point to assign to the same component as y^0.

Thus, there are eight total trees of length one in $\Gamma^{(2,2)}$

The length two trees in $\Gamma^{(2,2)}$ are maximal, so we can use Proposition 4.1 to calculate that there are $2^2 \cdot 2! = 8$ trees of length two.

Calculating the connections between simplices in $\Delta^{(2,2)}$ using edge contractions as described in the previous chapter, we find that $\Delta^{(2,2)}$ is a one-dimensional simplicial complex that is isomorphic to C_8, the cycle graph on eight vertices (see section 4.6.1).

4.4 Calculation of $\Gamma^{(3,2)}$ and $\Delta^{(3,2)}$

As in the previous section, these curves have two orbits of light marked points, so trees in $\Gamma^{(3,2)}$ will be either length one or two. Starting with the length one trees, similar to our calculation of length one tree in $\Gamma^{(2,2)}$ there are two options for what these trees could look like.

(1) We can assign both orbits to the outside components. In this case, there are three choices for each of the orbits of which of the three points to assign to the same component as y^0. Thus there are nine total trees of this type.

(2) Otherwise, we can assign one orbit to the central component and one orbit to the outside components. Then we have the choice of which of the two orbits to assign to the outside, as well as which of the three points in that orbit assign to the same component as y^0. Thus, there are six trees of this type.

Trees of length two are maximal, so we use Proposition 4.1 to calculate that there are $3^2 \cdot 2! = 18$ trees of length two.

Calculating the connections between simplices in $\Delta^{(3,2)}$ using edge contractions as described in the previous chapter, we find that $\Delta^{(3,2)}$ is a one-dimensional simplicial complex that is isomorphic the graph shown in section 4.6.2.

4.5 Calculation of $\Gamma^{(2,3)}$ and a partial calculation of $\Delta^{(2,3)}$

The curves in $\overline{\mathcal{L}}_3^2$ have three orbits of light marked points, so trees in $\Gamma^{(2,3)}$ are either length three, two, or one. Starting with length one trees, there are three options for what these trees could look like.

(1) If we assign all three orbits to the outside components, then there are two options for each of which of their points to assign to the same component as y^0. Thus, there are $2^3 = 8$ trees of this type.

(2) If we assign two orbits to the outside components and one orbit to the central component, then there are $\binom{3}{2}$ options for which two to assign to the outside components. Then, there are two options for each of those two orbits on which point to assign to the same component as y^0. Thus, there are $\binom{3}{2} \cdot 2^2 = 12$ trees of this type.

(3) If we assign one orbit of points to the outside components and the other two to the central components, then there are three options for which orbit to assign to the outside components. Then, for that orbit, there are two choices of the point that will be assigned to the same component as y^0. Thus, there are $3 \cdot 2 = 6$ length one trees of this type.

In total, there are 26 trees of length one in $\Gamma^{(2,3)}$. For length two trees, there are again three options as to what these trees could look like.

(1) We could assign one orbit to the outside components, one to the middle components, and one to the central component. There are 3! unique ways to make these assignments. Then, for the orbit on the middle and outside components, there are two choices for which point to assign to the same spoke as y^0. Thus, there are $3! \cdot 2^2 = 24$ length two trees of this type.

(2) Alternatively, we could assign two orbits to the outside components and one orbit to the middle components. There are $\binom{3}{2}$ ways to assign two orbits to the outside components. Then, for all three orbits, there are two choices for which point to assign to the same spoke as y^0. Thus, there are $\binom{3}{2} \cdot 2^3 = 24$ length two trees of this type.

(3) We could also assign two orbits to the middle components and one orbit to the outside components. This is the same calculation as (2), just with the middle and outside components switched. Thus, there are $\binom{3}{2} \cdot 2^3 = 24$ length two trees of this type.

In total, there are 72 trees on length two in $\Gamma^{(2,3)}$. Length three trees are maximal, so we can use Proposition 4.1 to calculate that there are $2^3 \times 3! = 48$ trees of length three in $\Gamma^{(2,3)}$.

Since $n = 3$, the dual boundary complex is a two-dimensional simplicial complex, which is harder to visualize than the graphs that we calculated in the previous sections, we provide a partial construction of $\Delta^{(2,3)}$ in section 4.6.3.

4.6 Figures

4.6.1 $\Gamma^{(2,2)}$ and $\Delta^{(2,2)}$

There are eight length one trees in $\Gamma^{(2,2)}$ which are shown below.

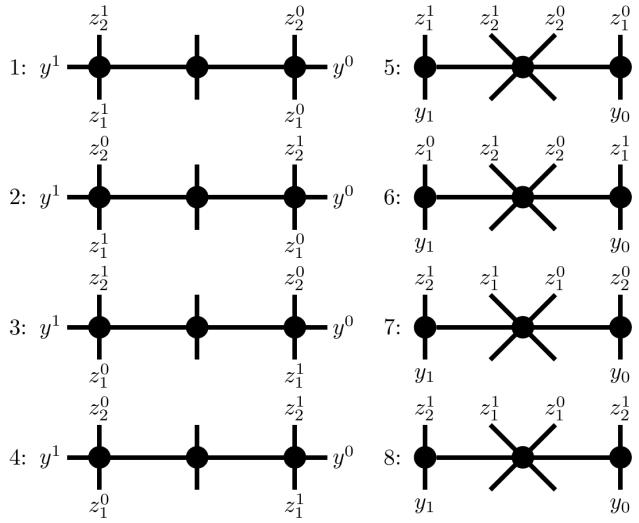

There are eight length two trees in $\Gamma^{(2,2)}$ which are shown and labeled below.

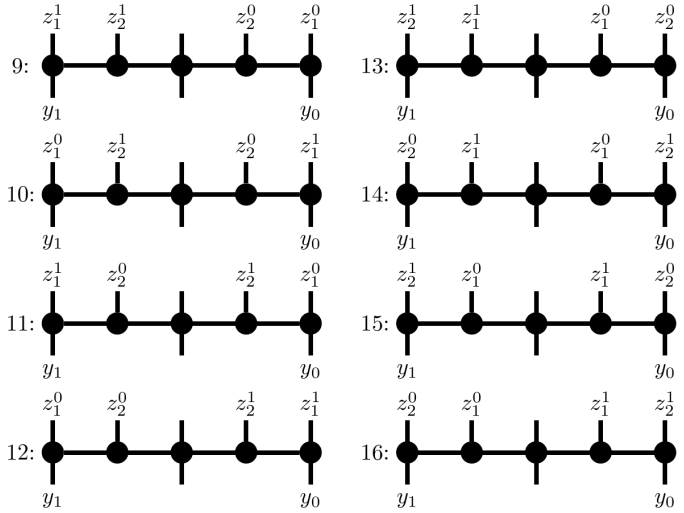

The dual boundary complex, $\Delta^{(2,2)}$ is isomorphic to the cycle graph on eight vertices, C_8. Labels on the simplices indicate their corresponding dual graphs as labeled in the images above.

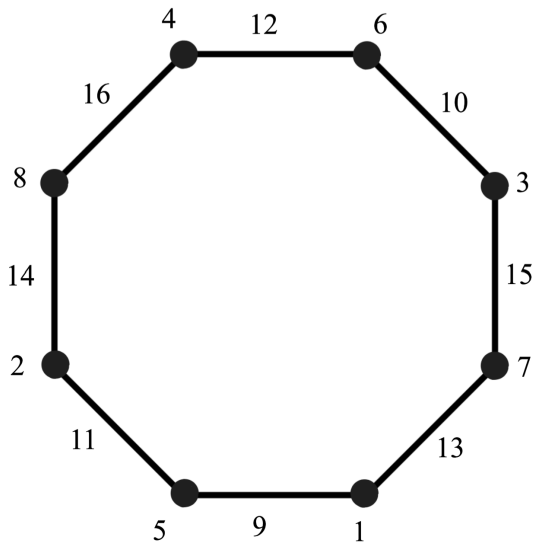

4.6.2 $\Gamma^{(3,2)}$ and $\Delta^{(3,2)}$

There are 15 length one trees in $\Gamma^{(3,2)}$ which are shown and labeled below.

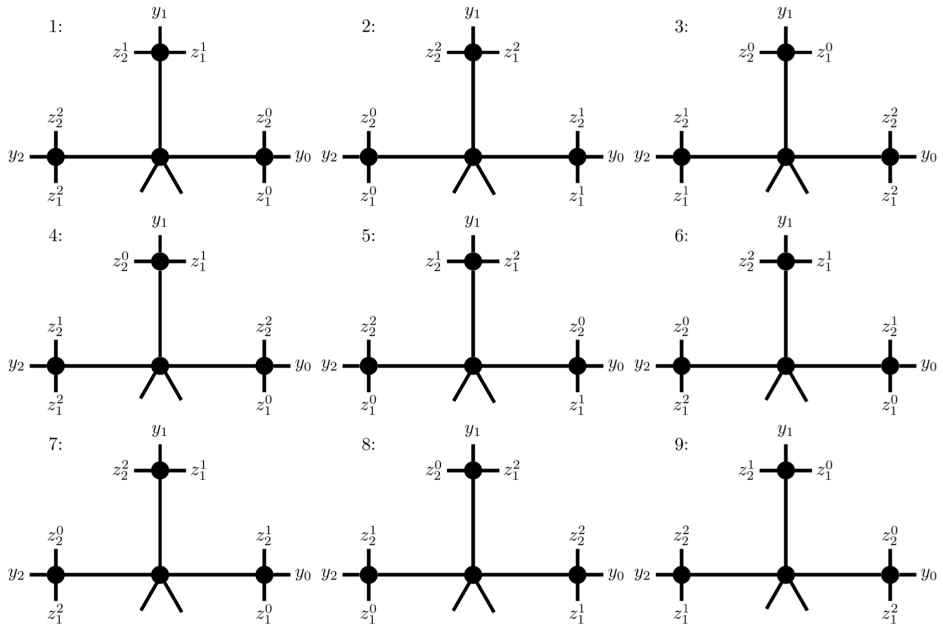

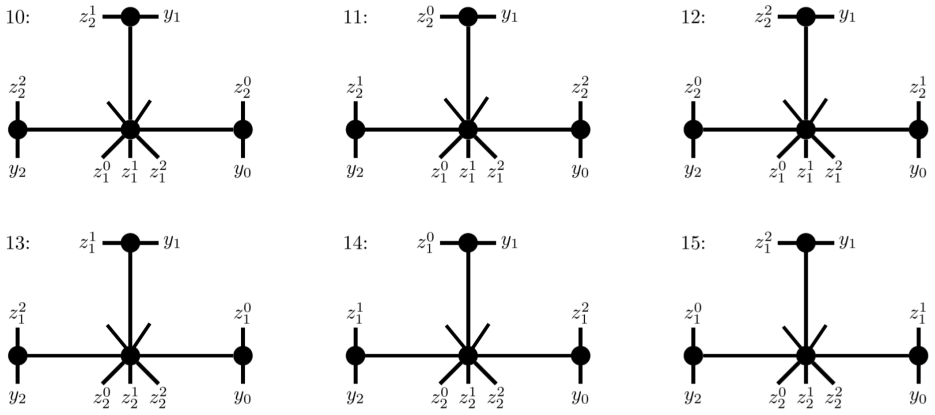

There are 18 length two trees in $\Gamma^{(3,2)}$ which are shown and labeled below.

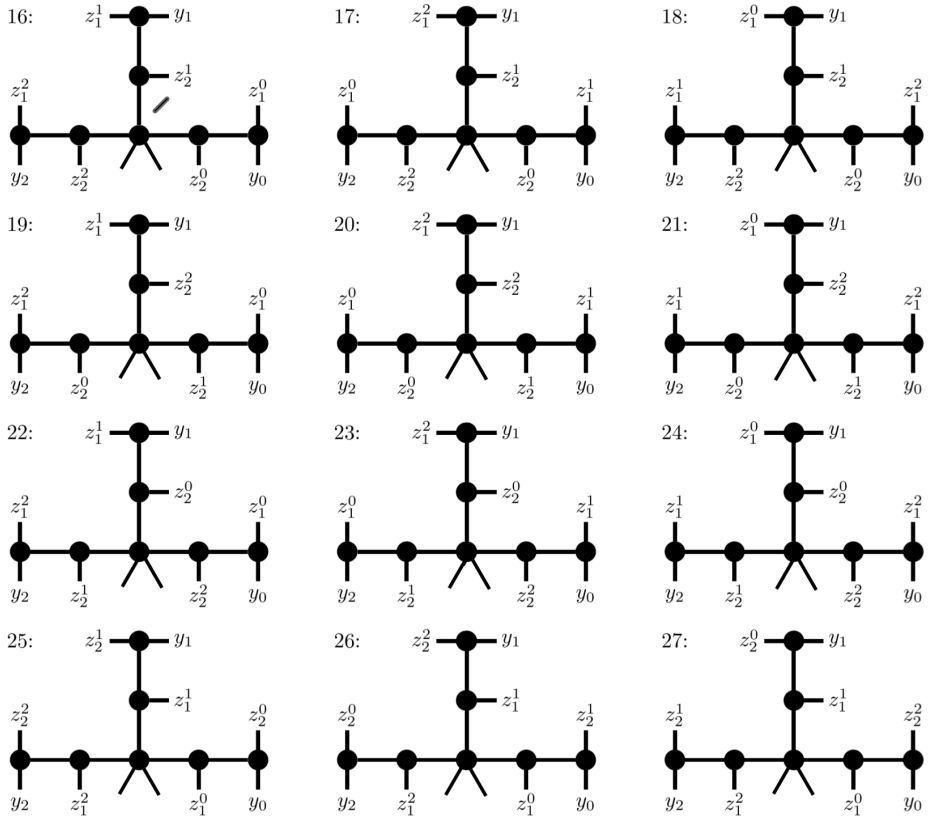

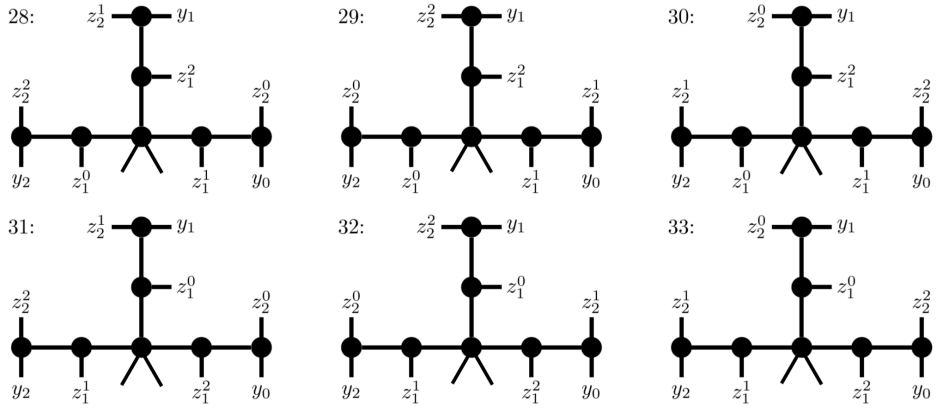

The dual boundary complex, $\Delta^{(3,2)}$, is a one-dimensional simplicial complex isomorphic to the graph shown below. Labels on the simplicies indicate their corresponding dual graphs as labeled above.

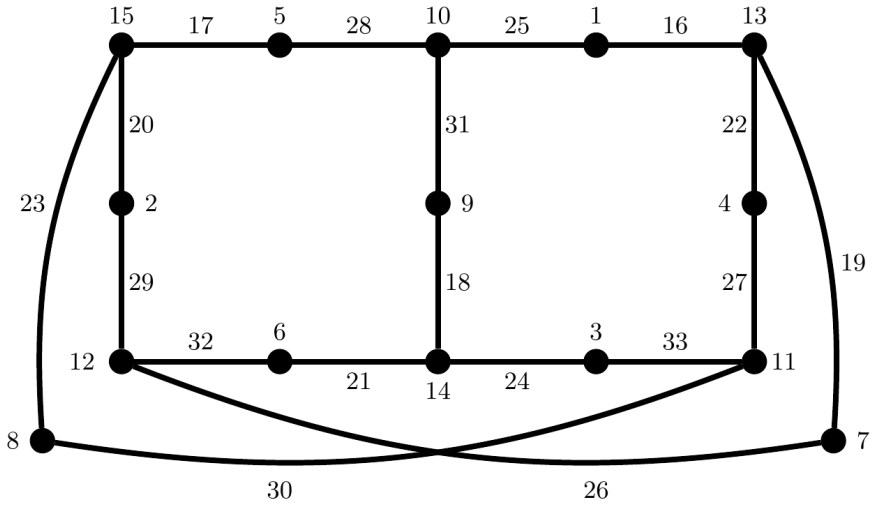

4.6.3 $\Gamma^{(2,3)}$ and $\Delta^{(2,3)}$

There are 48 length-three trees in $\Gamma^{(2,3)}$ which are shown and labeled below.

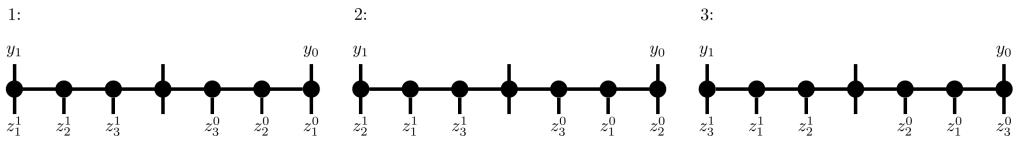

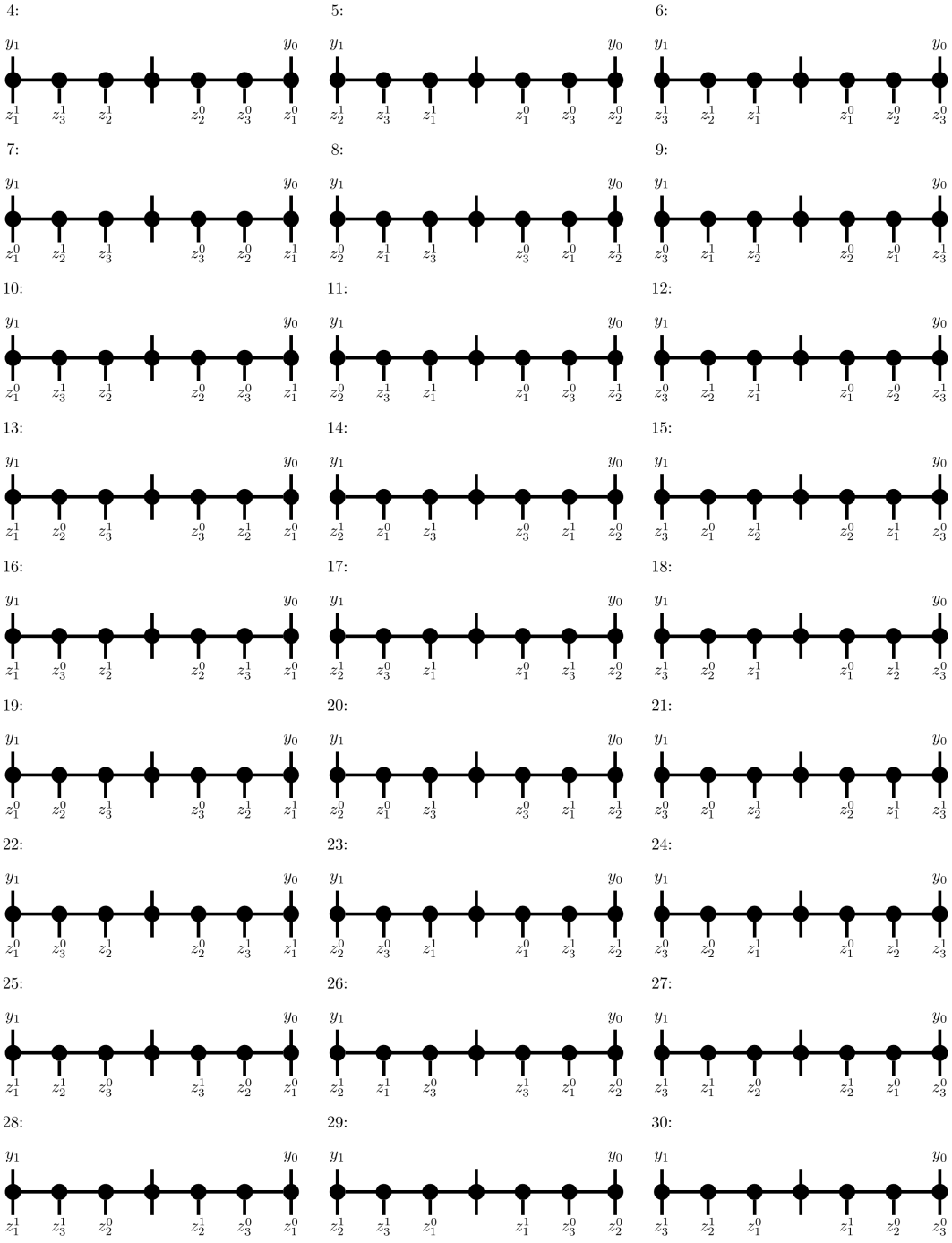
4:
y_1 y_0
z_1^1 z_3^1 z_2^1 z_2^0 z_3^0 z_1^0
5:
y_1 y_0
z_2^1 z_3^1 z_1^1 z_1^0 z_3^0 z_2^0
6:
y_1 y_0
z_3^1 z_2^1 z_1^1 z_1^0 z_2^0 z_3^0
7:
y_1 y_0
z_1^0 z_2^1 z_3^1 z_3^0 z_2^0 z_1^1
8:
y_1 y_0
z_2^0 z_1^1 z_3^1 z_3^0 z_1^0 z_2^1
9:
y_1 y_0
z_3^0 z_1^1 z_2^1 z_2^0 z_1^0 z_3^1
10:
y_1 y_0
z_1^0 z_3^1 z_2^1 z_2^0 z_3^0 z_1^1
11:
y_1 y_0
z_2^0 z_3^1 z_1^1 z_1^0 z_3^0 z_2^1
12:
y_1 y_0
z_3^0 z_2^1 z_1^1 z_1^0 z_2^0 z_3^1
13:
y_1 y_0
z_1^1 z_2^0 z_3^1 z_3^0 z_2^1 z_1^0
14:
y_1 y_0
z_2^1 z_1^0 z_3^1 z_3^0 z_1^1 z_2^0
15:
y_1 y_0
z_3^1 z_1^0 z_2^1 z_2^0 z_1^1 z_3^0
16:
y_1 y_0
z_1^1 z_3^0 z_2^1 z_2^0 z_3^1 z_1^0
17:
y_1 y_0
z_2^1 z_3^0 z_1^1 z_1^0 z_3^1 z_2^0
18:
y_1 y_0
z_3^1 z_2^0 z_1^1 z_1^0 z_2^1 z_3^0
19:
y_1 y_0
z_1^0 z_2^0 z_3^1 z_3^0 z_2^1 z_1^1
20:
y_1 y_0
z_2^0 z_1^0 z_3^1 z_3^0 z_1^1 z_2^1
21:
y_1 y_0
z_3^0 z_1^0 z_2^1 z_2^0 z_1^1 z_3^1
22:
y_1 y_0
z_1^0 z_3^0 z_2^1 z_2^0 z_3^1 z_1^1
23:
y_1 y_0
z_2^0 z_3^0 z_1^1 z_1^0 z_3^1 z_2^1
24:
y_1 y_0
z_3^0 z_2^0 z_1^1 z_1^0 z_2^1 z_3^1
25:
y_1 y_0
z_1^1 z_2^1 z_3^0 z_3^1 z_2^0 z_1^0
26:
y_1 y_0
z_2^1 z_1^1 z_3^0 z_3^1 z_1^0 z_2^0
27:
y_1 y_0
z_3^1 z_1^1 z_2^0 z_2^1 z_1^0 z_3^0
28:
y_1 y_0
z_1^1 z_3^1 z_2^0 z_2^1 z_3^0 z_1^0
29:
y_1 y_0
z_2^1 z_3^1 z_1^0 z_1^1 z_3^0 z_2^0
30:
y_1 y_0
z_3^1 z_2^1 z_1^0 z_1^1 z_2^0 z_3^0

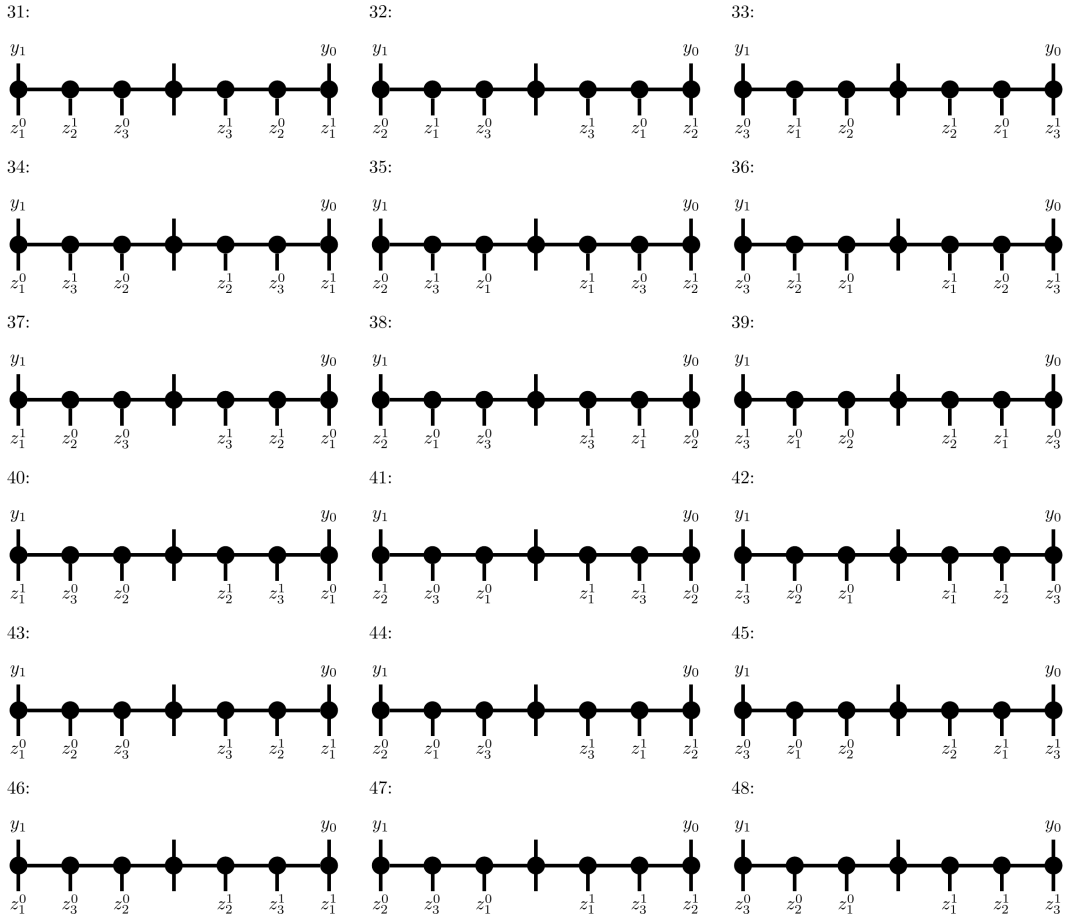

There are 72 length-two trees in $\Gamma^{(2,3)}$ which are shown and labeled below.

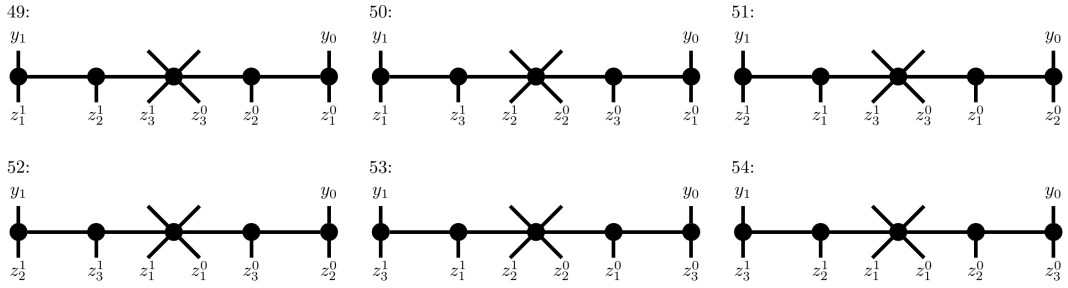

55:
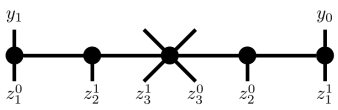

56:
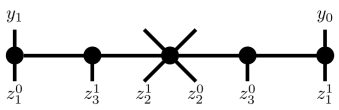

57:
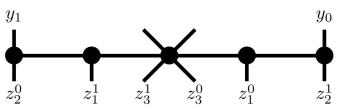

58:
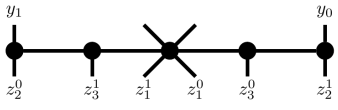

59:
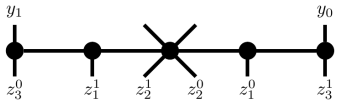

60:
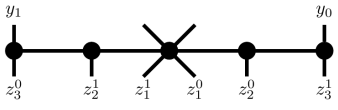

61:
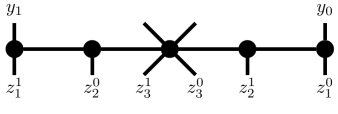

62:
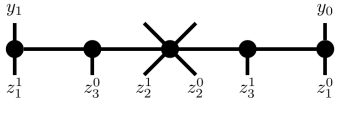

63:
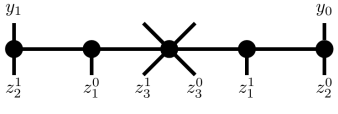

64:
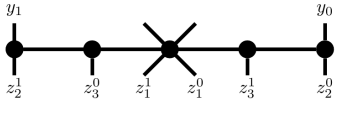

65:
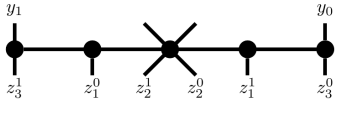

66:
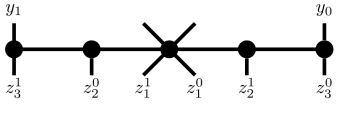

67:
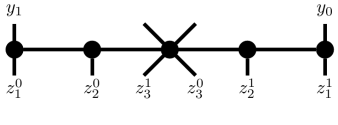

68:
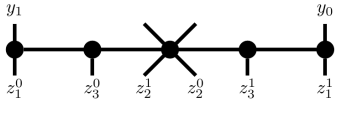

69:
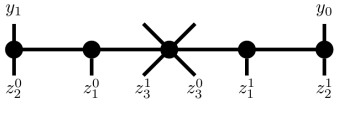

70:
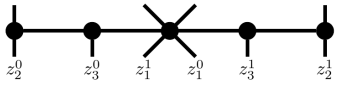

71:
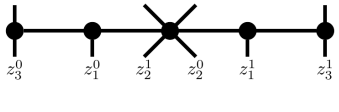

72:
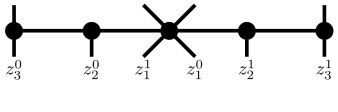

73:
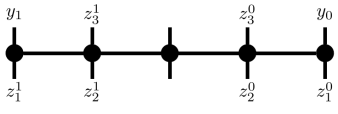

74:
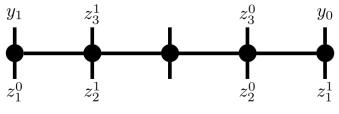

75:
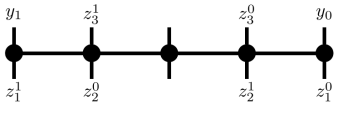

76:
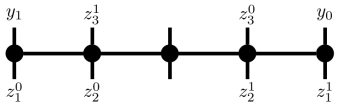

77:
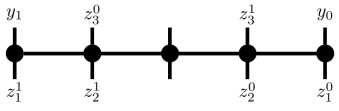

78:
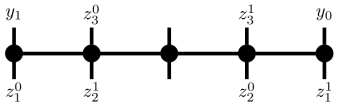

79:
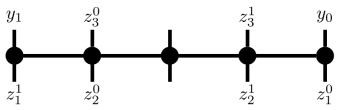

80:
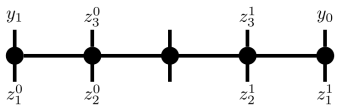

81:
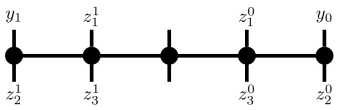

82:
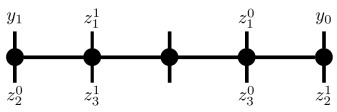

83:
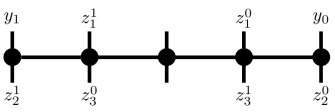

84:
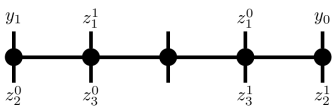

85:
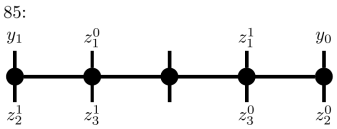

86:
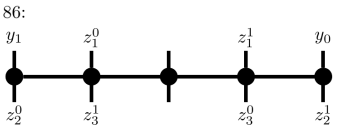

87:
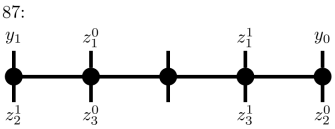

88:
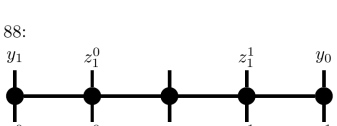

89:
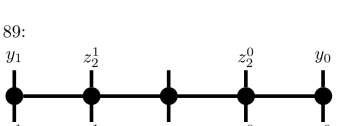

90:
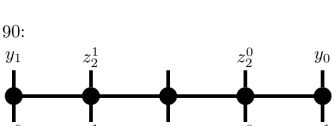

91:
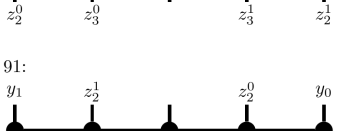

92:
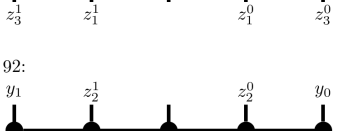

93:
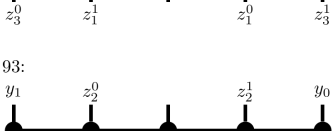

94:


95:


96:


97:
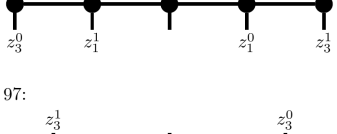

98:
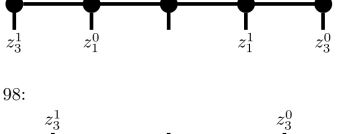

99:
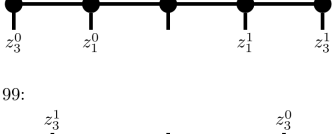

100:
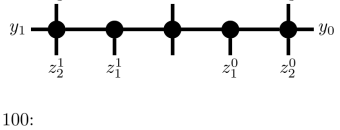

101:
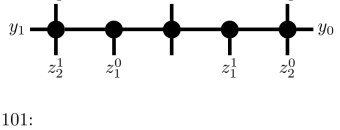

102:
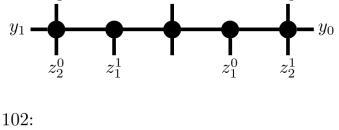

103:
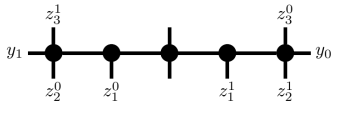

104:
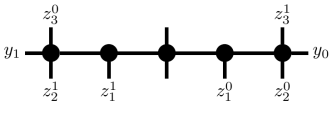

105:
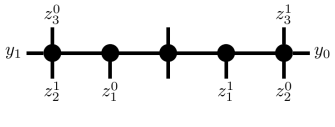

106:
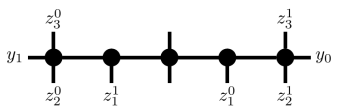

107:
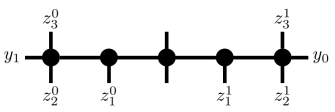

108:
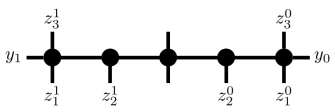

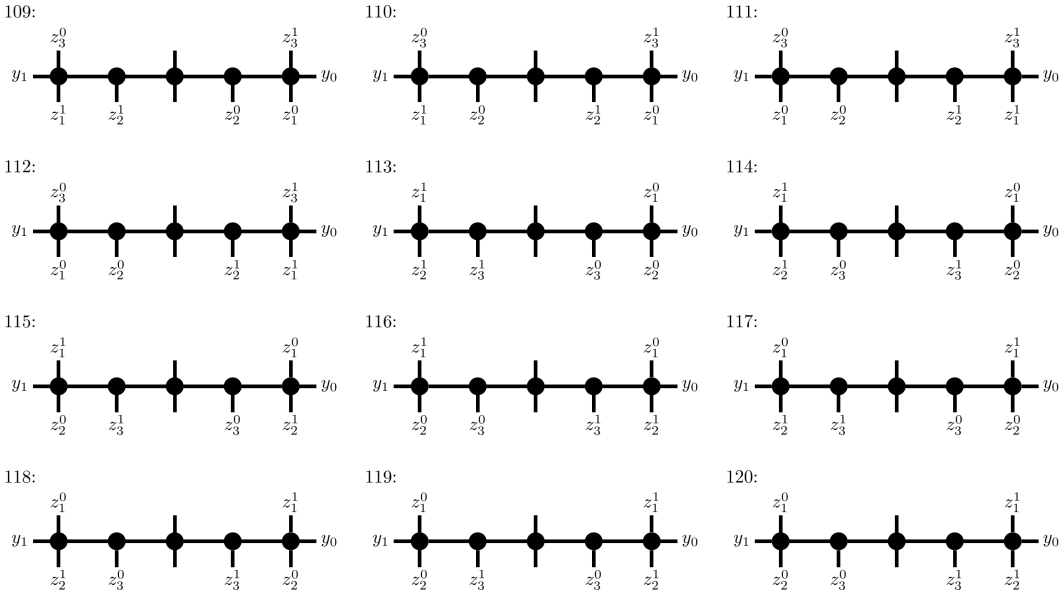

There are 26 length-one trees in $\Gamma^{(3,2)}$ which are shown and labeled below.

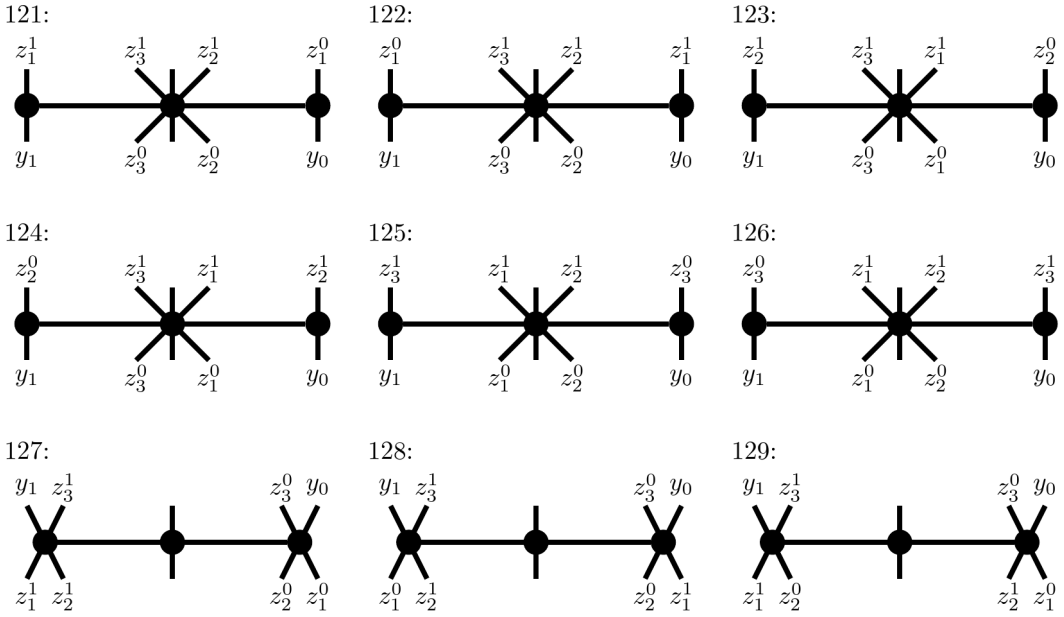

130:

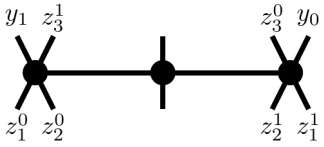

131:

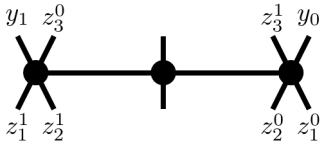

132:

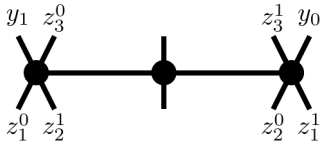

133:

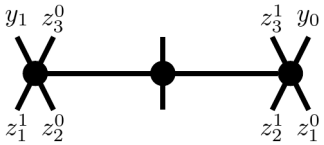

134:

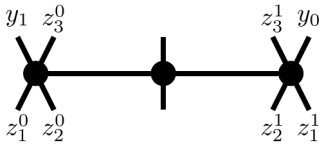

135:

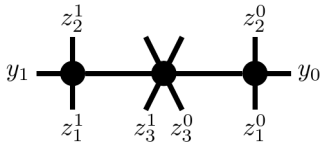

135:

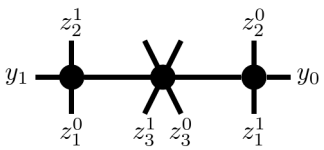

137:

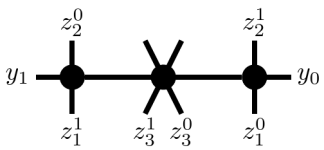

138:

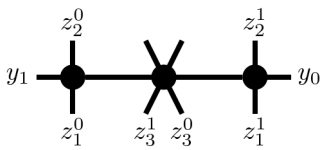

139:

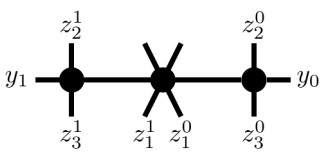

140:

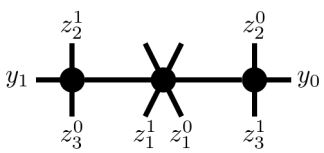

141:

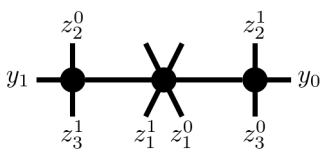

142:

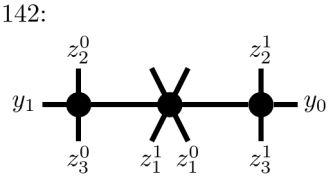

143:

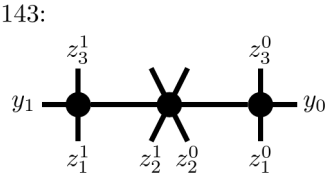

144:

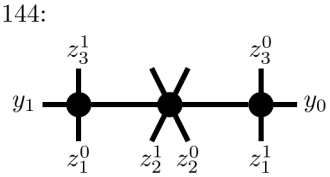

145:

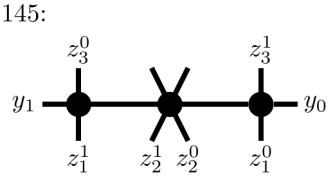

146:

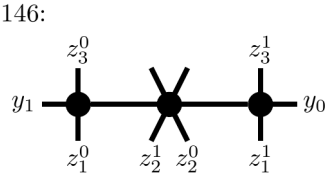

The dual boundary complex, $\Delta^{(2,3)}$, is a two-dimensional simplicial complex. We provide a partial construction by calculating the maximal simplices and their faces. Labels on simplicies indicate their corresponding dual graph as labeled above.

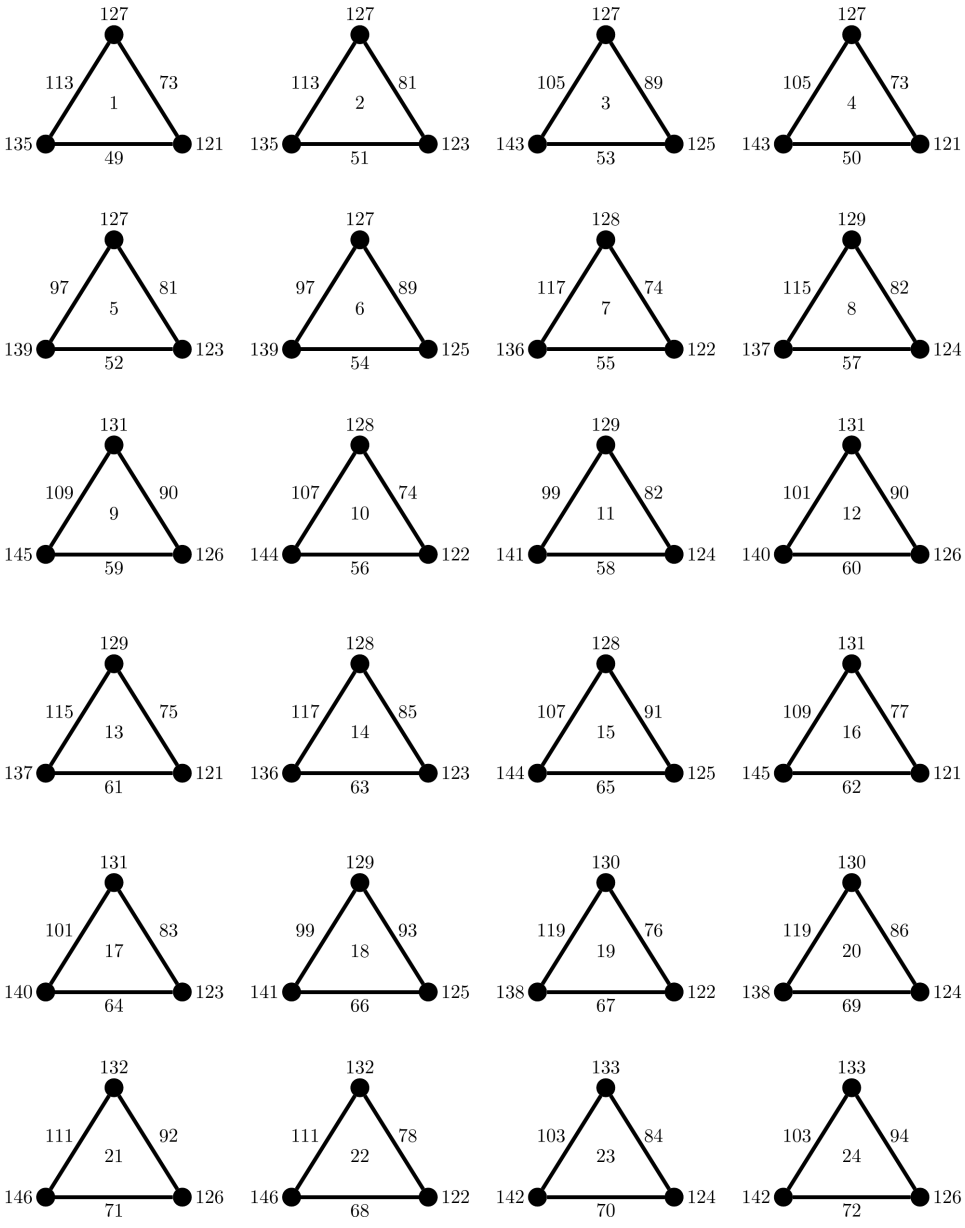

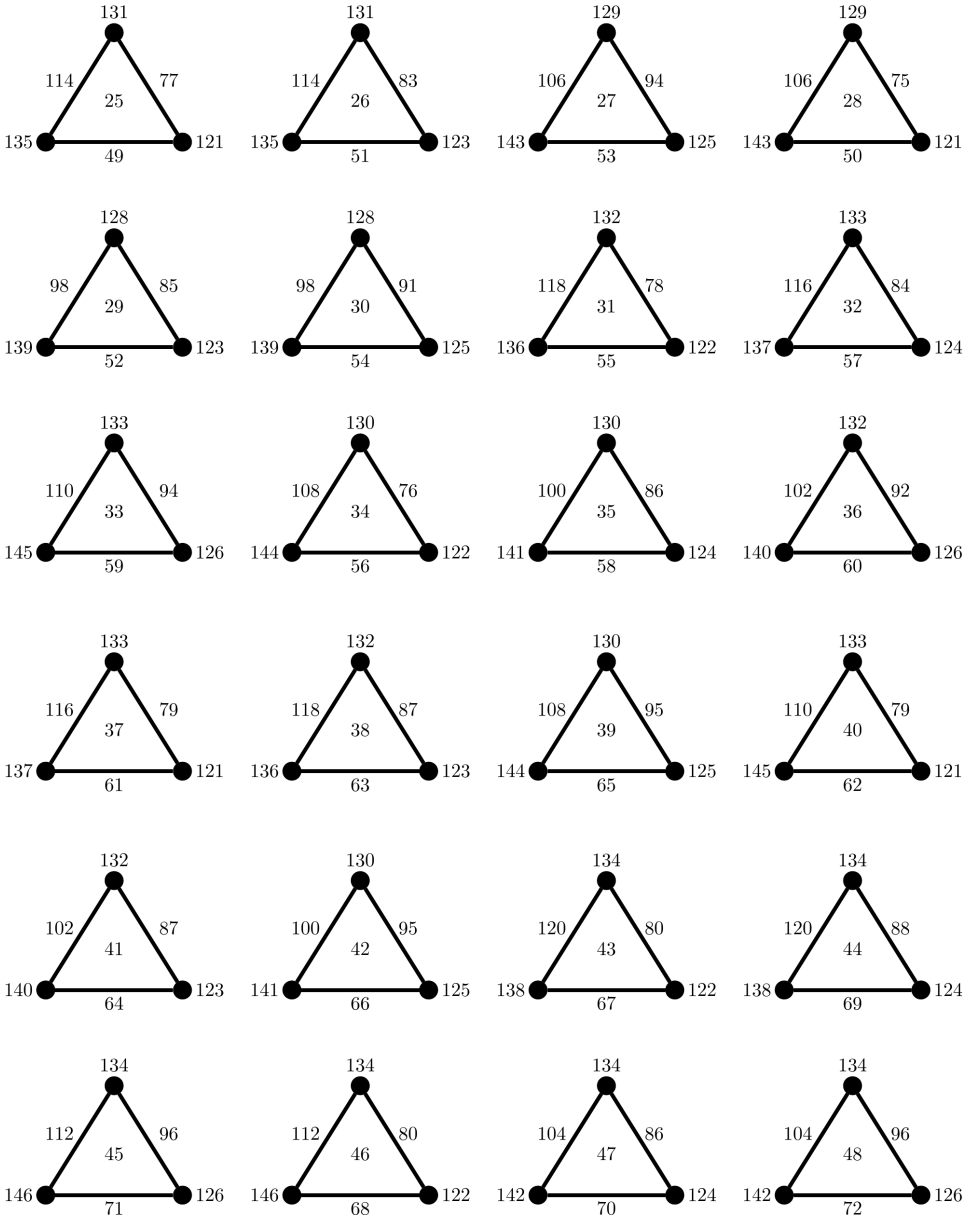
131
114
77
25
135
121
49
131
114
83
26
135
123
51
129
106
94
27
143
125
53
129
106
75
28
143
121
50
128
98
85
29
139
123
52
128
98
91
30
139
125
54
132
118
78
31
136
122
55
133
116
84
32
137
124
57
133
110
94
33
145
126
59
130
108
76
34
144
122
56
130
100
86
35
141
124
58
132
102
92
36
140
126
60
133
116
79
37
137
121
61
132
118
87
38
136
123
63
130
108
95
39
144
125
65
133
110
79
40
145
121
62
132
102
87
41
140
123
64
130
100
95
42
141
125
66
134
120
80
43
138
122
67
134
120
88
44
138
124
69
134
112
96
45
146
126
71
134
112
80
46
146
122
68
134
104
86
47
142
124
70
134
104
96
48
142
126
72

Chapter 5

Euler Characteristic of $\Delta^{(r,n)}$

In this chapter, we use combinatorial techniques to compute the Euler characteristic of $\Delta^{(r,n)}$. An introduction to the Euler characteristic is provided in Chapter 1, but to summarize, the Euler characteristic is a topological invariant that is defined for simplicial complexes as follows.

Definition 5.1. *Let X be a finite simplicial complex and let $X[k]$ be the set of k-dimensional simplices in X. Then, the Euler characteristic of X is defined as*

$$\chi(X) = \sum_{k=0}^{dim(X)} (-1)^k |X[k]|.$$

In other words, it is the alternating sum of the number of m-dimensional simplices in X for all $m = 0, 1, \ldots, dim(X)$.

By deriving a generating function for the number of k-dimensional simplices in $\Delta^{(r,n)}$, we are able to prove that

$$\chi(\Delta^{(r,n)}) = 1 - (1 - r)^n.$$

5.1 Recursive Relation for $|\Delta^{(r,n)}[k]|$

Since the Euler characteristic is the alternating sum of the number of k-dimensional simplices in a given simplicial complex, we need a way to count the number of k-dimensional simplices in $\Delta^{(r,n)}$. This is equivalent to counting the number of length-$(k+1)$ trees in $\Gamma^{(r,n)}$. To do this, we define the following relation that is recursive on n:

Proposition 5.1. *Let $r, n > 0$ and $-1 \leq k \leq n$, and let $|\Delta^{(r,n)}[k]|$ denote the number of k-dimensional simplices in $\Delta^{(r,n)}$. Then, the following recursive relationship on n holds.*

$$|\Delta^{(r,n)}(k)| = r(1+k)|\Delta^{(r,n-1)}[k-1]| + (r(k+1)+1)|\Delta^{(r,n-1)}[k]|. \tag{5.1}$$

Proof. Since k-dimensional simplices correspond to length $k+1$ trees in $\Gamma^{(r,n)}$, (5.1) equivalently counts the number of length $k+1$ trees in $\Gamma^{(r,n)}$. Let T be some length $k+1$ tree in $\Gamma^{(r,n)}$. We want to count the ways in which we can obtain T by adding an orbit to a tree in $\Gamma^{(r,n-1)}$. We have two base cases.

(1) When $k = -1$, $|\Delta^{(r,n)}[-1]| = 1$. This base case corresponds to a tree of length 0, of which there is only one for all r, n (each marked point leaf is incident to the center node).

(2) When $n = 0$, $|\Delta^{(r,n)}[k] = 0$. This base case corresponds to a tree with no orbits of light points. Unless $k = -1$, there are no stable trees of this form.

We proceed in cases.

- *Case 1*: Let T_1 be a length k tree in $\Gamma^{(r,n-1)}$. To obtain a length $k+1$ tree, we must choose a corresponding vertex on each spoke from which to extend another edge and vertex. There are $k+1$ options for this, as we could choose any of the k vertices on a given spoke or the center vertex. This new vertex will only have two incident edges, so to meet the stability conditions, we must add an n^{th} orbit, $z_n^0, \ldots, z_n^{r-1}$ to these vertices. Choose one of the r new vertices to ascribe z_n^0. Then, the rest are determined by the automorphism σ. Thus, there are $r(k+1)$ unique ways to create T from T_1 and $|\Delta^{(r,n-1)}[k-1]|$ possible T_1 from which to choose.

- *Case 2*: Let T_2 be a length $k+1$ tree in $\Gamma^{(r,n-1)}$. Then, we can choose a vertex on which to add z_n^0. Then, $z_n^1, \ldots, z_n^{r-1}$ will be sent to vertices according to the automorphism σ. There are $r(k+1)+1$ vertices on T_2. Thus, there are $(r(k+1)+1)$ unique ways to create T from T_2, and $|\Delta^{(r,n-1)}(k)|$ possible T_2 from which to choose.

Adding these two cases together, we see that $|\Delta^{(r,n)}(k)| = r(1+k)|\Delta^{(r,n-1)}(k-1)| + (r(k+1)+1)|\Delta^{(r,n-1)}(k)|$ as desired. □

Figure 5.1 illustrates this proof by showing how we can get a length 3 tree in $\Gamma^{(3,4)}$ from a length 2 and a length 3 tree in $\Gamma^{(3,3)}$

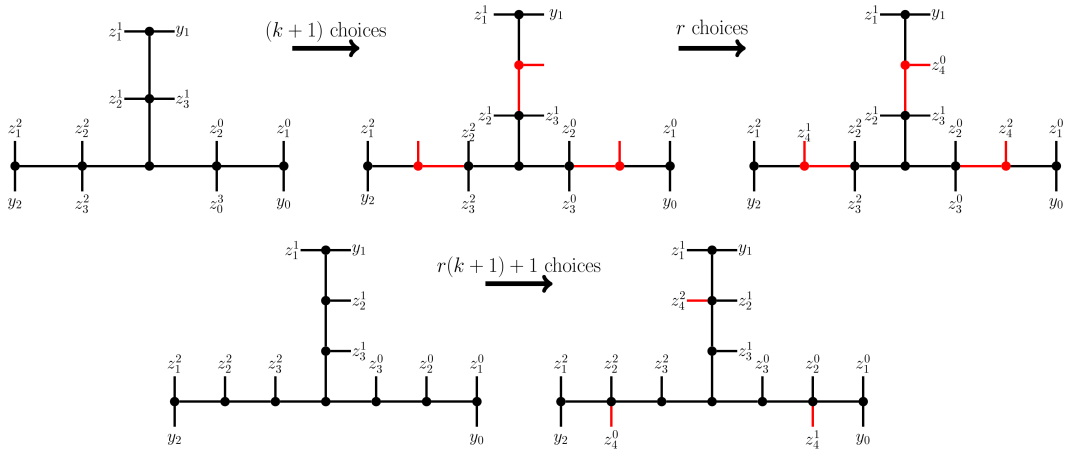

Figure 5.1 The two methods in which we can create a length 3 tree in $\Gamma^{(3,4)}$ from trees in $\Gamma^{(3,3)}$.

5.2 Generating Function for $|\Delta^{(r,n)}[k]|$

Now that we have defined a recursive relation that counts the number of k-dimensional simplices in $\Delta^{(r,n)}$, we will use this to obtain a generating function.

Definition 5.2. *A generating function is a way to represent the elements of an infinite sequence as coefficients of a formal power series.*

In our case, the coefficients represent $|\Delta^{(r,n)}|$ where r and k are fixed and n increases with each term. We define both an ordinary and exponential generating function, the latter of which will be used in our final proof of the Euler characteristic.

5.2.1 "Ordinary" Generating Function

Define the generating function by

$$F_{r,k}(x) = \sum_{n=1}^{\infty} |\Delta^{(r,n)}[k]| x^n. \tag{5.2}$$

The coefficient of the x^n term of this power series represents the number of k-dimensional simplices in $\Delta^{(r,n)}$. Multiplying (5.2) by $x(r(k+1)+1)$ we get

$$\begin{aligned} x(r(k+1)+1)F_{r,k}(x) &= x(r(k+1)+1)\sum_{n=1}^{\infty}|\Delta^{(r,n)}[k]|x^n \\ &= (r(k+1)+1)\sum_{n=1}^{\infty}|\Delta^{(r,n)}[k]|x^{n+1}. \end{aligned}$$

Reindexing, we get

$$(r(k+1)+1)\sum_{n=1}^{\infty}|\Delta^{(r,n)}[k]|x^{n+1} = (r(k+1)+1)\sum_{n=2}^{\infty}|\Delta^{(r,n-1)}[k]|x^n$$

Now, we have a generating function that for which the coefficients are k-dimensional simplices in $\Delta^{(r,n-1)}$. Similarly, we can multiply $F_{r,k-1}(x)$ by $x(k+1)r$ to get

$$\begin{aligned} x(k+1)rF_{r,k-1}(x) &= x(k+1)r\sum_{n=1}^{\infty}|\Delta^{(r,n)}[k-1]|x^n \\ &= (k+1)r\sum_{n=2}^{\infty}|\Delta^{(r,n-1)}[k-1]|x^n \end{aligned}$$

which provides us with a generating function that counts the number of $(k-1)$-dimensional simplices in $\Delta^{(r,n-1)}$. Motivated by (5.1), we define the following equation for $F_{r,k}(x)$:

$$F_{k,r}(x) = x(k+1)rF_{r,k-1}(x) + x(r(k+1)+1)F_{r,k}(x).$$

Solving for $F_{r,k}(x)$ yields

$$F_{r,k}(x) = \frac{x(k+1)r}{1-x(r(k+1)+1)}F_{r,k-1}(x). \tag{5.3}$$

Proposition 5.2. *$F_{r,k}(x)$ has non-recursive solution*

$$F_{r,k}(x) = \left(\prod_{n=1}^{k+1}\frac{rnx}{1-x(rn+1)}\right)\cdot\frac{1}{1-x}. \tag{5.4}$$

Proof. Let $|\Delta^{(r,n)[-1]}|$ be the number of length 0 trees in $\Gamma^{(r,n)}$. For all r, n, $|\Delta^{(r,n)[-1]}| = 1$, where every marked point lies on one central component. Note that this tree is not included in our construction of $\Delta^{(r,n)}$ (there is no such thing as a -1 degree simplex), but it provides a useful initial condition for (5.3). Then, we can define

$$\begin{aligned} F_{-1,r}(x) &= \sum_{n=0}^{\infty} |\Delta^{(r,n)}[-1]| x^n \\ &= \sum_{n=0}^{\infty} x^n \\ &= \frac{1}{1-x} \end{aligned}$$

With this initial condition, we proceed with a proof by induction. For the base case, let $k = 0$. Then, from (5.3) we know

$$\begin{aligned} F_{(r,0)}(x) &= \frac{xr}{1-x(r+1)} F_{r,-1}(x) \\ &= \frac{xr}{1-x(r+1)} \cdot \frac{1}{1-x} \\ &= \left(\prod_{n=1}^{1} \frac{rnx}{1-x(rn+1)} \right) \cdot \frac{1}{1-x}. \end{aligned}$$

as desired. Thus, the base case holds. Assume that for $k = j$, it holds that

$$F_{r,j}(x) = \left(\prod_{n=1}^{j+1} \frac{rnx}{1-x(rn+1)} \right) \cdot \frac{1}{1-x}.$$

From (5.3), we know that

$$\begin{aligned} F_{r,j+1}(x) &= \frac{x(j+2)r}{1-x(r(j+2)+1)} F_{r,j}(x) \\ &= \frac{x(j+2)r}{1-x(r(j+2)+1)} \cdot \left(\prod_{n=1}^{j+1} \frac{rnx}{1-x(rn+1)} \right) \cdot \frac{1}{1-x} \\ &= \left(\prod_{n=1}^{j+2} \frac{rnx}{1-x(rn+1)} \right) \cdot \frac{1}{1-x} \end{aligned}$$

as desired. Thus, the inductive step holds and Proposition 5.2 holds for all r and k. □

5.2.2 Exponential Generating Function

Define the exponential generating function by

$$F^{\exp}_{r,k}(x) = \sum_{n=1}^{\infty} |\Delta^{(r,n)}[k]| \frac{x^n}{n!}. \tag{5.5}$$

Similar to the "ordinary" generating function, the coefficients of $\frac{x^n}{n!}$ in this power series represent the number of k-dimensional simplices in $\Delta^{(r,n)}$. Taking the integral of (5.5), we get

$$\begin{aligned}\int F^{\exp}_{r,k}(x)dx &= \int \sum_{n=1}^{\infty} |\Delta^{(r,n)}[k]| \frac{x^n}{n!} dx \\ &= \sum_{n=1}^{\infty} \frac{1}{n+1} |\Delta^{(r,n)}[k]| \frac{x^{n+1}}{n!} \\ &= \sum_{n=1}^{\infty} |\Delta^{(r,n)}[k]| \frac{x^{n+1}}{n+1!}.\end{aligned}$$

Then, re-indexing, we get

$$\int F^{\exp}_{r,k}(x)dx = \sum_{n=2}^{\infty} |\Delta^{(r,n-1)}[k]| \frac{x^n}{n!}.$$

Similar to the process used with the ordinary generating function, we can use these calculations to rewrite (5.1) in terms of the exponential generating function as so:

$$F^{\exp}_{r,k}(x)dx = r(1+k) \int F^{\exp}_{r,k-1}(x)dx + (r(k+1)+1) \int F^{\exp}_{r,k}(x)dx.$$

Differentiating both sides, we get

$$\frac{d}{dx} F^{\exp}_{r,k}(x) = r(k+1) F^{\exp}_{r,k-1}(x) + (r(k+1)+1) F^{\exp}_{r,k}(x), \tag{5.6}$$

which is a first-order differential equation.

Proposition 5.3. *By solving the differential equation given by* (5.6)*, we get*

$$F^{exp}_{r,k}(x) = \sum_{n=0}^{k+1} (-1)^{k-n+1} \binom{k+1}{n} e^{nrx+x} \tag{5.7}$$

as a non-recursive solution for $F^{exp}_{r,k}(x)$.

Proof. Let $|\Delta^{(r,n)[-1]}|$ be the number of length 0 trees in $\Gamma^{(r,n)}$. For all r, n, $|\Delta^{(r,n)[-1]}| = 1$, where every marked point lies on one central component. Note that this tree is not included in our construction of $\Delta^{(r,n)}$ (there is no such thing as a -1 degree simplex), but it provides a useful initial condition for (5.6). Then, we can define

$$\begin{aligned} F^{\exp}_{r,-1}(x) &= \sum_{n=0}^{\infty} |\Delta^{(r,n)}[-1]| \frac{x^n}{n!} \\ &= \sum_{n=0}^{\infty} \frac{x^n}{n!} \\ &= e^x. \end{aligned}$$

We now proceed by induction. For the base case, let $k = 0$. Additionally, for simplicity of notation, let $y = F^{\exp}_{r,0} =$ Then, we know from (5.7) that

$$y' = re^x + (1 + r)y.$$

We can solve this first-order differential equation using the integrating factor method. Our integrating factor is

$$\mu = e^{\int -(1-r)dx} = e^{-rx-x}.$$

Multiplying through by μ, we get

$$e^{-(rx+x)}y' - e^{-(rx+x)}(1 + r)y = -re^{-rx}.$$

Then, integrating both sides, we get

$$\begin{aligned} \int (e^{-(rx+x)}y' - e^{-(rx+x)}(1 + r)y)dx &= \int -re^{-rx}dx \\ e^{-(rx+x)}y &= e^{-rx} + C \\ y &= Ce^{rx+x} - e^x. \end{aligned}$$

To determine C, we use the base case $|\Delta^{(r,0)}[k] = 0$. In our generating function, $n = 0$ corresponds to the constant term, so when we plug in $x = 0$ to $F_{r,k}(x)$, we should get 0. Thus,

$$0 = C - 1,$$

so $C = 1$. Then, we check

$$y = e^{rx+x} - e^x = \sum_{n=0}^{1} (-1)^{1-n} \binom{1}{n} e^{nrx+x}$$

as desired, so the base case holds. Now, assume that for $k = j - 1$, it holds that

$$F_{r,j-1}(x)^{\exp} = \sum_{n=0}^{j} (-1)^{j-n} \binom{j}{n} e^{nrx+x}.$$

Then, let $k = j$. Again, for simplicity of notation, let $y = F_{r,j}^{\exp}$. The differential equation for y given by (5.6) is

$$y' = r(j+1) \sum_{n=0}^{j} (-1)^{j-n} \binom{j}{n} e^{nrx+x} + (r(j+1)+1)y.$$

Again, we solve this using the integrating factor method. Our integrating factor is

$$\mu = e^{-\int (r(j+1)+1)dx} = e^{-xr(j+1)-x}.$$

Multiplying through by μ, we get

$$\mu y' - \mu(r(j+1)+1)y = \left(r(j+1) \sum_{n=0}^{j} (-1)^{j-n} \binom{j}{n} e^{nrx+x} \right) e^{-xr(j+1)-x}.$$

Then, integrating both sides,

$$\int (\mu y' - \mu(r(j+1)+1)y)\, dx = \int \left(r(j+1) \sum_{n=0}^{j} (-1)^{j-n} \binom{j}{n} e^{nrx+x} \right) e^{-xr(j+1)-x} dx$$

$$e^{-rx(j+1)-x} y = \int \left(r(j+1) \sum_{n=0}^{j} (-1)^{j-n} \binom{j}{n} e^{nrx+x} \right) e^{-rx(j+1)-x} dx.$$

Because our sum is finite, we can swap the integral and the sum. We can also pull μ into the sum since it does not depend on n. Then,

$$\begin{aligned} e^{-rx(j+1)-x} y &= r(j+1) \sum_{n=0}^{j} \int (-1)^{j-n} \binom{j}{n} e^{nrx-(j+1)x} dx \\ &= r(j+1) \sum_{n=0}^{j} (-1)^{j-n} \binom{j}{n} \int e^{nrx-(j+1)x} dx \end{aligned}$$

$$= r(j+1)\sum_{n=0}^{j}(-1)^{j-n}\binom{j}{n}\frac{1}{rn-r(j+1)}e^{nrx-(j+1)x} + C$$

$$= \sum_{n=0}^{j}(-1)^{j-n}\binom{j}{n}\frac{r(j+1)}{rn-r(j+1)}e^{nrx-(j+1)x} + C$$

$$= \sum_{n=0}^{j}(-1)^{j-n}\binom{j+1}{n}e^{nrx-(j+1)x} + C.$$

Multiplying each side by $e^{rx(j+1)+x}$, we get

$$y = \sum_{n=0}^{j}(-1)^{j-n}\binom{j+1}{n}e^{nrx+x} + Ce^{rx(j+1)+x}. \tag{5.8}$$

To determine C, use the base case that $|\Delta^{(r,0)}[k]| = 0$. In our exponential generating function, $n = 0$ corresponds to the constant term, so when we plug in $x = 0$ to $F^{\exp}_{r,k}(x)$, we should get 0. So,

$$0 = \sum_{n=0}^{j}(-1)^{j-n}\binom{j+1}{n} + C.$$

By the binomial theorem,

$$(-1+1)^{j+1} = \sum_{n=0}^{j+1}\binom{j+1}{n}(-1)^{j+1-n}(1)^n$$

$$0 = \sum_{n=0}^{j+1}\binom{j+1}{n}(-1)^{j+1-n}.$$

Dividing both sides by -1,

$$0 = \sum_{n=0}^{j+1}\binom{j+1}{n}(-1)^{j-n}$$

$$= \sum_{n=0}^{j}(-1)^{j-n}\binom{j+1}{n} + \binom{j+1}{j+1}(-1)^{j-j+1}$$

$$= \sum_{n=0}^{j}(-1)^{j-n}\binom{j+1}{n} - 1.$$

Thus, we have shown

$$\sum_{n=0}^{j}(-1)^{j-n}\binom{j+1}{n}+C=\sum_{n=0}^{j}(-1)^{j-n}\binom{j+1}{n}-1,$$

so $C=-1$. Plugging this into 5.8, we get

$$\begin{aligned}y&=\sum_{n=0}^{j}(-1)^{j-n}\binom{j+1}{n}e^{nrx+x}-e^{rx(j+1)+x}\\&=\sum_{n=0}^{j+1}(-1)^{j+1-n}\binom{j+1}{n}e^{nrx+x}\end{aligned}$$

as desired. Thus, the inductive step holds, and Proposition 5.3 is true for all r and k. □

5.3 Calculation of the Euler Characteristic

With a non-recursive solution for the exponential generating function of $|\Delta^{(r,n)}[k]|$, we are now ready to prove the Euler characteristic of $\Delta^{(r,n)}$. Remember that the formula for the Euler characteristic is

$$\chi(\Delta^{(r,n)})=\sum_{k=0}^{n-1}(-1)^k|\Delta^{(r,n)}[k]|.$$

In the previous sections, we defined an exponential generating function $F^{\exp}_{r,k}(x)$ for $|\Delta^{(r,n)}[k]|$, so by taking the alternating sum of the coefficients of $F^{\exp}_{r,k}(x)$, we obtain an exponential generating function in which the coefficients are the Euler characteristic of $\Delta^{(r,n)}$ for given r where n increases with each term. Let

$$G^{\exp}_{r}(x)=\sum_{k=0}^{\infty}(-1)^kF^{\exp}_{r,k}(x)$$

be this generating function.

We'll first present a lemma that will be useful in our proof of the Euler characteristic.

Lemma 5.1. *Let $u=e^x$. Then,*

$$F^{exp}_{r,k}(x)=u(u^r-1)^{k+1}.$$

Proof. By the binomial theorem,

$$\begin{aligned} u(u^r-1)^{k+1} &= \sum_{n=0}^{k+1} \binom{k+1}{n} (u^r)^n (-1)^{k+1-n} \\ &= \sum_{n=0}^{k+1} (-1)^{k+1-n} \binom{k+1}{n} (u^r)^n \cdot u \\ &= \sum_{n=0}^{k+1} (-1)^{k+1-n} \binom{k+1}{n} (u^r)^n \cdot u^{rn+1} \\ &= F_{r,k}^{\exp}(x) \end{aligned}$$

as desired. □

Theorem 5.1. *The Euler characteristic of $\Delta^{(r,n)}$ is given by*

$$\chi(\Delta^{(r,n)}) = 1-(1-r)^n.$$

Proof. We calculate a non-recursive solution for $G_r^{\exp}(x)$. By lemma 5.1,

$$\begin{aligned} G_r^{\exp}(x) &= \sum_{k=0}^{\infty} u(u^{r-1})^{k+1} \\ &= \frac{1}{1+(u^{r-1})} \cdot u(u^{r-1}) \\ &= \frac{u(u^{r-1})}{u^r}. \end{aligned}$$

Now, reversing our change of variables and replacing u with e^x, we get

$$\begin{aligned} \frac{u(u^{r-1})}{u^r} &= \frac{e^x(e^{rx}-1)}{e^{rx}} \\ &= \frac{e^{rx+x}-e^x}{e^{rx}} \\ &= e^x - e^{(1-r)x}. \end{aligned}$$

Now, our conjecture is that $\chi(\Delta^{(r,n)}) = 1-(1-r)^n$. This has exponential generating function

$$\begin{aligned} \sum_{n=0}^{\infty} (1-(1-r)^n)\frac{x^n}{n!} &= e^{(1-(1-r))x} \\ &= e^x - e^{(1-r)x}. \end{aligned}$$

The exponential generating function for the Euler characteristic, G_r, and the exponential generating function for our conjectured result are equivalent. Thus,

$$\chi(\Delta^{(r,n)}) = 1 - (1 - r)^n$$

as desired. □

Chapter 6

Homotopy Type of $\Delta^{(r,n)}$

In this chapter, we provide a conjecture for the homotopy type for $\Delta^{(r,n)}$. While we will not prove this conjecture, we explore two possible proof techniques: contractible subcomplexes and shellings.

Homotopy type is introduced in Chapter 1, but as a summary, it is a property of topological spaces that provides insight into the space's general structure. If two spaces have the same homotopy type (i.e. they are homotopy equivalent), we may continuously deform one space into the other by compressing, dilating, and translating its parts, but without "cutting", "gluing", or "ripping" its parts.

Definition 6.1. *A homotopy between two continuous functions f, g from topological space X to topological space Y is a continuous function $h : X \times [0,1]$ such that $H(x,0) = f(x)$ and $H(x,1) = g(x)$ for all $t \in [0,1]$.*

Two topological spaces X and Y are homotopy equivalent if there exists two continuous maps $f : X \to Y$ and $g : Y \to X$ such that $f \circ g$ is homotopic to the identity map on Y and $g \circ f$ is homotopic to the identity map on X.

Before presenting the conjecture on the homotopy type of $\Delta^{(r,n)}$, we introduce a few important definitions.

Definition 6.2. *Let X and Y be two topological spaces with points x_0 and y_0 respectively. The wedge sum of X and Y, denotes $X \vee Y$, is the disjoint union of X and Y where x_0 is identified with y_0, i.e.*

$$X \vee Y = (X \sqcup Y)/\sim$$

where $x_0 \sim y_0$. In other words, the wedge sum of X and Y obtained by gluing X and Y together at a single point.

This definition can be extended to any number of finite topological spaces.

Our conjecture for the homotopy type of $\Delta^{(r,n)}$ involves the wedge sum of spheres, also called a *bouquet of spheres*.

Example 6.1. *Let X and Y both be circles. Then, $X \vee Y$ is given by a figure-eight.*

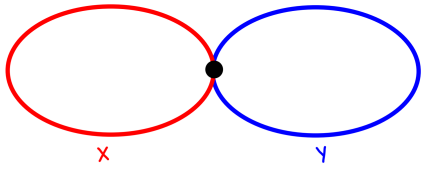

Figure 6.1 The wedge sum of two circles

Conjecture 6.1. *The homotopy type of $\Delta^{(r,n)}$ is a wedge sum of $(r-1)^n$ spheres of dimension $n-1$.*

To gain some evidence for why this might be true, we can look at two brief examples.

Example 6.2. *Take $\Delta^{(2,2)}$, which is isomorphic to C_8, the cycle graph on eight vertices. It is not too difficult to imagine how, by rounding out the edges, we could continuously deform $\Delta^{(2,2)}$ into the wedge sum of one sphere of degree 1 (i.e. a circle, see figure 5.2).*

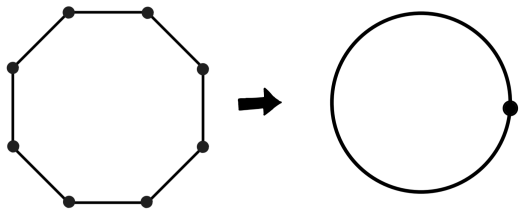

Figure 6.2 $\Delta^{(2,2)}$ is homotopy equivalent to the wedge sum of one circle.

Example 6.3. *Consider $\Delta^{(3,2)}$. This graph contains 4 cycles. We can imagine continuously deforming $\Delta^{(3,2)}$ to a bouquet of four one-dimensional spheres by rounding out the edges and shrinking some of the edges until the four cycles meet at a single point.*

Additionally, our result for the Euler characteristic of $\Delta^{(r,n)}$ provides evidence that our conjecture of the number of spheres in the wedge sum is

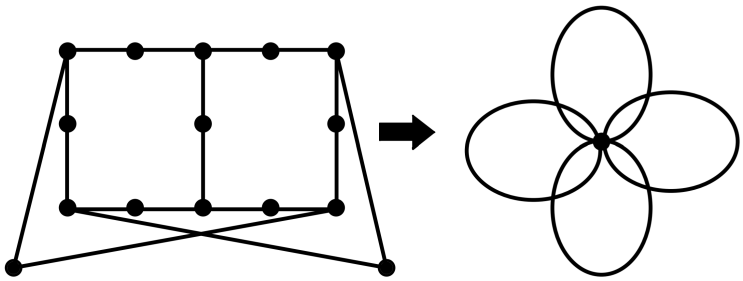

Figure 6.3 $\Delta^{(3,2)}$ is homotopy equivalent to a wedge sum of four circles.

correct. Since it is a topological invariant, the Euler characteristic of $\Delta^{(3,2)}$ and the wedge sum of spheres of dimension $(n-1)$ should be equal.

Let $W_{m,k}$ denote the wedge sum of k spheres of dimension m. It is known that $\chi(W_{m,k}) = 1 + (-1)^m k$ (nLab authors (2024)). So, setting this (where $m = n-1$) equal to our result for the Euler characteristic of $\Delta^{(r,n)}$, we can solve for k.

$$\begin{aligned} 1 - (1-r)^n &= 1 + (-1)^{n-1} k \\ -(1-r)^n &= (-1)^{n-1} k \end{aligned}$$

Multiplying both sides by -1,

$$\begin{aligned} (1-r)^n &= (-1)^n k \\ k &= \frac{(1-r)^n}{(-1)^n} \\ &= (r-1)^n \end{aligned}$$

Thus, we expect that the number of spheres in each wedge sum will be $(r-1)^n$.

6.1 Approach 1: Contractible Subcomplexes

This approach is inspired by Robinson and Whitehouse (1996), who were able to prove that the space of fully grown trees, T_n, is homotopy equivalent to a wedge sum of spheres of dimension $n-3$. This space is very closely

related to $\Gamma_{0,n}$; in fact, $T_n \cong \Gamma_{0,n+1}$, the set of dual graphs of curves in $\overline{\mathcal{M}}_{0,n+1}$. Robinson and Whitehouse prove this using the idea of contractible subcomplexes.

Definition 6.3. *A topological space is contractible if it is homotopy equivalent to a point. In other words, the space can be continuously deformed to a single point.*

Example 6.4. *Consider topological spaces in that resemble the letters A and G. The letter G is contractible because it could be continuously shrunk to a single point. The letter A, however, is not contractible. Notice that, since A has a hole, we can not continuously deform it to a single point without ripping points apart or gluing points together to close the hole.*

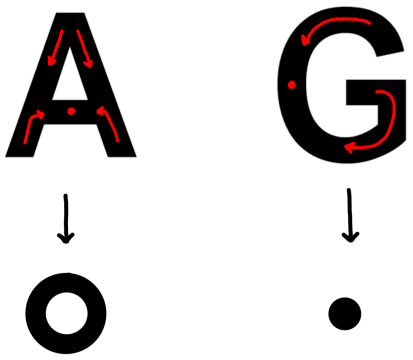

Robinson and Whitehouse defined subcomplexes of T_n that were contractible and proved that their union is either also contractible or empty, Thus, the union of these contractible subcomplexes are also contractible, and contracting this union leaves a space that is homotopy equivalent to a wedge of spheres of dimension $n-3$.

Our conjectural approach for proving the homotopy type of $\Delta^{(r,n)}$ using contractible subcomplexes is the same. We want to 1) find contractible subcomplexes of $\Delta^{(r,n)}$, 2) prove that their non-empty intersections must also be contractible, and 3) prove that when the union of those subcomplexes are contracted, the result is homotopy equivalent to a wedge of spheres of dimension $n-1$.

To find these contractible subcomplexes, we consider subsets of trees in $\Gamma^{(r,n)}$ that are defined by a property that is closed under edge contraction.

Example 6.5. *Consider $\Gamma^{(3,2)}$. Figure 5.3 shows the subset of seven trees for which z_0^1 is on the same node as y_1. We claim that this subset is closed under edge*

contraction, and that all of these trees can contract to tree 14 *(as labeled in section* 4.6.2*).*

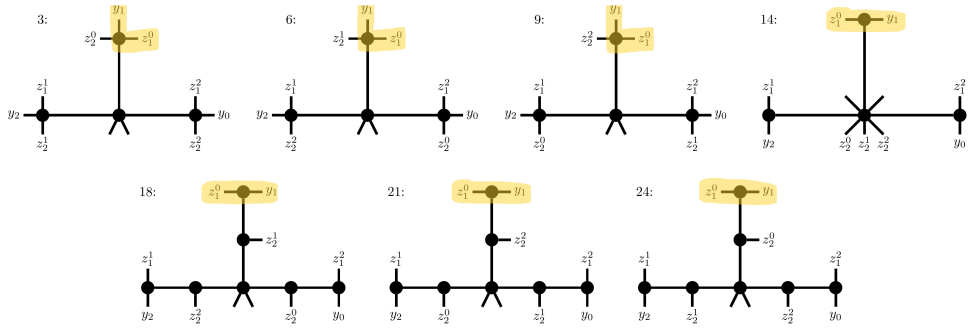

Figure 6.4 The subset of $\Gamma^{(3,2)}$ for which z_1^0 and y_1 are on the same node.

Then, by assigning a metric to each of the edges in these trees, we can define a function on this metric that will continuously deform each tree into tree 14*. For trees that are length two in this subset (e.g. tree* 24 *as shown in figure* 6.5*), assign metric* $x \in [0,1]$ *to the inside edge on each spoke and metric* $1-x$ *to the outside edge on each spoke. Then, on interval* $t \in [0,1]$*, we can continuously deform the inside edges with* $x(1-t)$ *and the outside edges with* $(1-x)+tx$*. At time* $t = 1$*, the inside edges and outside edges will have their metric equal to zero and one respectively. Recall from Definition* 3.4 *that we consider an edge with metric equal to zero to be equivalent to that edge being contracted. Thus, tree* 24 *contracts to tree* 14 *as desired.*

Trees that are length one in this subset (e.g. tree 9 *as labeled in figure* 6.4*), are considered to be equivalent to length* 2 *trees for which one of the orbits of edges is assigned a metric of zero. Thus, for tree* 9*, we can separate* y_i *and* z_1^i *from* z_2^i *on each spoke with an edge with metric equal to zero. The inside edges are thus assigned a metric of one. Then, similar to above, on the interval* $t \in [0,1]$*, we can continuously deform the inside edges with* $(1-t)$ *and the outside edges with* t*. At time* $t = 1$*,the inside edges and outside edges will have metric equal to zero and one respectively. Thus, tree* 9 *contracts to tree* 14 *as desired (see figure* 6.5*).*

Now, we know this subset of trees is contractible to tree 14*, so their corresponding simplices on* $\Delta^{(3,2)}$ *must form a contractible subcomplex that contracts to the vertex representing tree* 14*. This is shown in figure* 6.6*.*

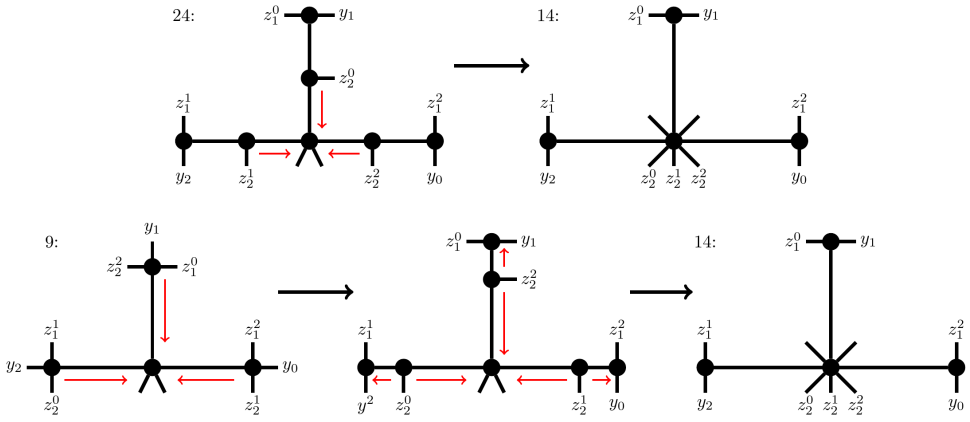

Figure 6.5 Each tree in this subset can be contracted to tree 14.

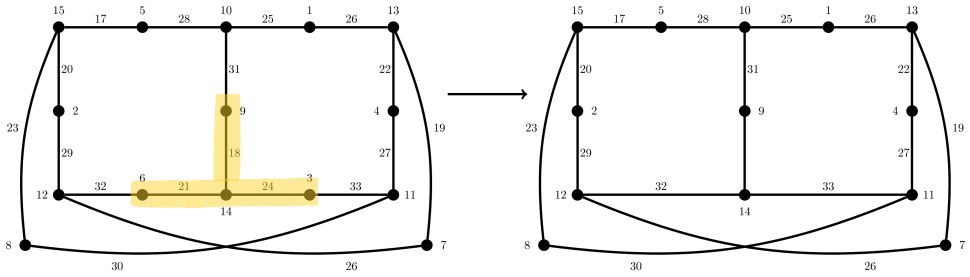

Figure 6.6 A contractible subcomplex on $\Delta^{(r,n)}$.

6.2 Approach 2: Shelling

We start this approach by introducing a few important definitions.

Definition 6.4. *A k-dimensional simplicial complex is called pure if its maximal simplices all have dimension k.*

Definition 6.5. *Let X be a finite or countably infinite simplicial complex and let $C_1, C_2, \ldots$ be an ordering of the maximal simplicies of X. Then, this ordering is a shelling if the complex*

$$B_j = \left(\bigcup_{i=1}^{j-1} C_i \right) \cap C_j$$

is pure and of dimension $\dim C_j - 1$ for all $j = 2, 3, \ldots$. If B_j is the entire boundary of C_j, then C_j is called spanning.

A simplicial complex that admits a shelling is called *shellable*. It is known

that if a simplicial complex is shellable, then it is homotopy equivalent to a wedge sum of spheres (one for each spanning simplex of corresponding dimension) (Francisco et al. (2014)). Thus, to find the homotopy type of $\Delta^{(r,n)}$ using this approach, we want to find a procedure that will produce a shelling for any $\Delta^{(r,n)}$.

Example 6.6. *Consider $\Delta^{(3,2)}$. Its maximal simplices are of dimension one (edges). Figure 6.7 shows the edges labeled C_1 through C_{18}. We can see that for all $j = 1, \ldots, 18$, C_j either intersects the previously labeled edges at one vertex or two, the latter of which makes C_j a spanning simplex. Either way, each B_j is a pure simplicial complex, so this labeling admits a shelling.*

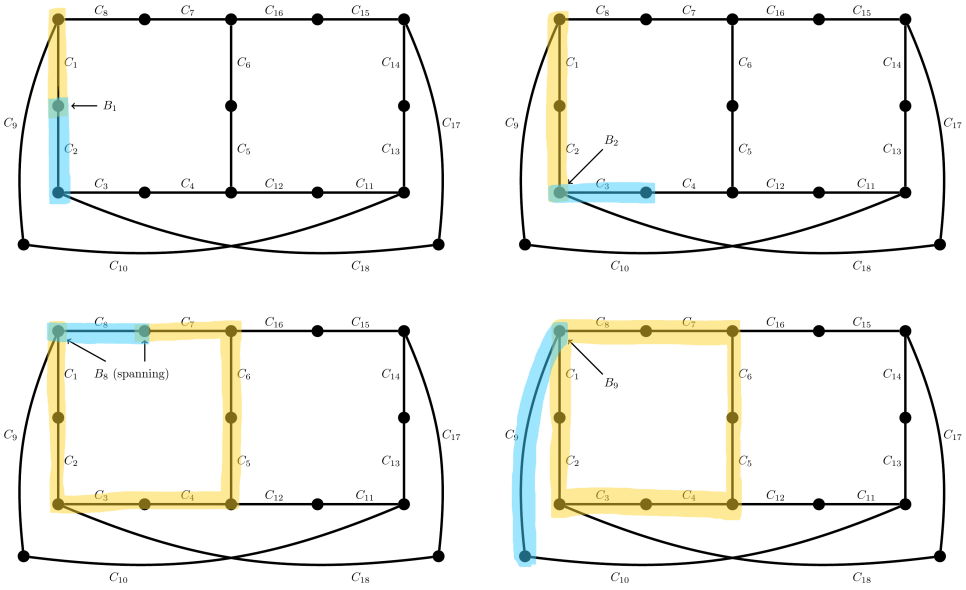

Figure 6.7 The labelling of the edges of $\Delta^{(3,2)}$ above admits a shelling.

There are multiple possible shellings for any given $\Delta^{(r,n)}$.

Example 6.7. *All of the labellings shown in figure 6.8 are shellings of $\Delta^{(r,n)}$ (in this figure, the C is dropped and each maximal simplex is labeled with just a number). The spanning simplices are highlighted. We see that for each, there are four spanning simplices. Thus, as conjectured in Example 6.3, $\Delta^{(3,2)}$ is homotopy equivalent to a wedge sum of four spheres of dimension one (i.e. four circles).*

We conjecture that it is sufficient that if the next maximal simplex you label is adjacent to one that has already been labeled, then the resulting labeling will be a shelling.

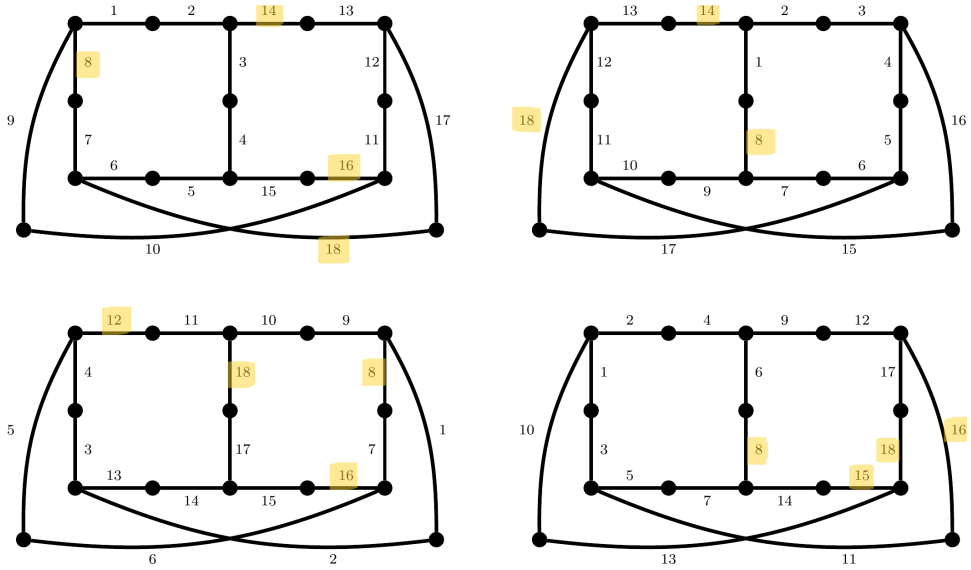

Figure 6.8 Four shellings of $\Delta^{(3,2)}$ with spanning simplices highlighted.

To get a procedural labeling of the maximal simplicies in $\Delta^{(r,n)}$, one approach we tried was to "swap" pairs of orbits on the maximal trees in $\Gamma^{(r,n)}$. For example, in $\Gamma^{2,3}$, consider the 2-simplex that corresponds to the following length 3 tree to be C_1.

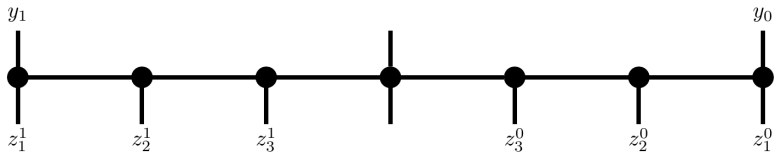

Then, we can swap the components to which z_1^i and z_2^i are incident, resulting in the following length three tree, whose corresponding two-simplex we label as the next maximal simplex in our shelling C_2.

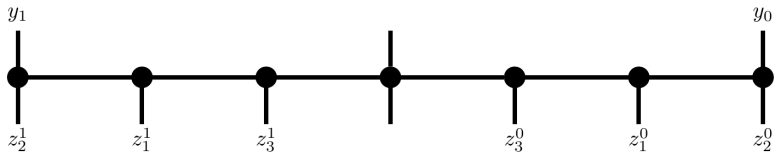

This kind of swapping and labeling procedure guarantees that C_i and C_{i+1} are adjacent simplices in $\Delta^{(r,n)}$ which we conjectured above as being sufficient for a shelling. Figure 6.7 shows the steps of a specific swapping procedure we tried, in which we cycle through swapping the outer two components, inner two components, and center two components. However, this procedure ultimately did not work. Any labeling procedure needs to hit *all* of the maximal simplicies before hitting repeats. Otherwise, some maximal simplicies will never be labeled. This causes challenges when complexes contain many cycles, as this kind of swapping procedure often takes us around one of the cycles and we are forced to repeat a simplex before covering them all.

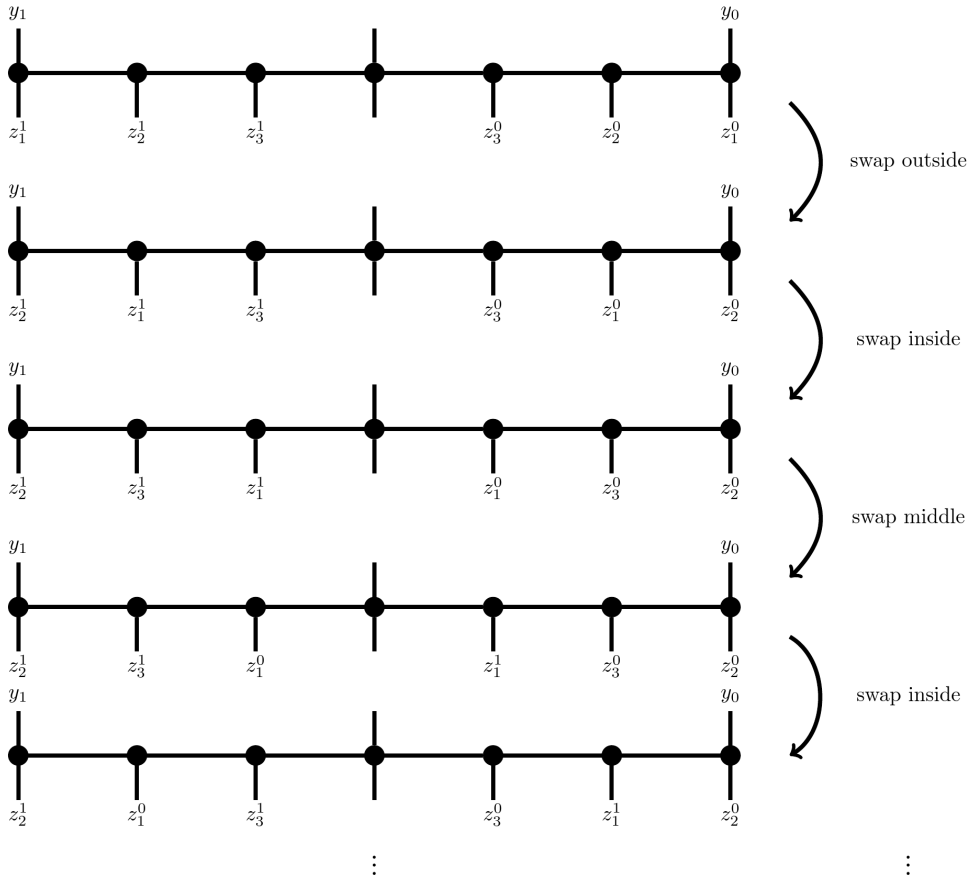

Figure 6.9 Swapping procedure that results in adjacent simplicies.

For example, $\Delta^{(3,2)}$ is a graph with no Eulerian path (i.e. a path that visits

every edge exactly once with repeat visits to vertices allowed). Thus, the swapping procedure described above will not work for $\Delta^{(3,2)}$.

As of yet, we have not been able to find a procedural way to label the maximal simplicies of $\Delta^{(r,n)}$ such that C_i and C_{i+1} are always adjacent and all maximal simplicies are covered.

Chapter 7

Future Work

In this chapter, discuss next steps for calculating the homotopy type and leave you with some questions about $\Delta^{(r,n)}$ that might be interesting to explore in the future work.

7.1 Homotopy Type

The most immediate future work is to prove the conjecture of the homotopy type of $\Delta^{(r,n)}$ using one (or both) of the two methods presented in chapter 6.

If using the contractible subcomplexes approach, we need to find a way to construct $\Delta^{(r,n)}$ as a union of contractible subcomplexes for all r, n, such that the intersection of these subcomplexes are either empty or also contractible. Then, we will know $\Delta^{(r,n)}$ is itself contractible, and must show it contracts to a wedge sum of $(r-1)^n$ spheres of dimension $n-1$.

With the shelling approach, any procedure that provides a valid shelling for any r, n (i.e. a sequence of adjacent maximal simplices in $\Delta^{(r,n)}$ such that each maximal simplex is covered once) will immediately prove the desired result.

7.2 Other Interesting Questions

In addition to the Euler characteristic and homotopy type, there are a few other characteristics of $\Delta^{(r,n)}$ that would be interesting to investigate.

7.2.1 Automorphism Group

Calculating the homotopy type of $\Delta^{(r,n)}$ will provide a lot of information about its general structure, but there are properties that we cannot learn from its homotopy type. For example, what are the symmetries of $\Delta^{(r,n)}$? This motivates future work into calculating the automorphism group of $\Delta^{(r,n)}$

Definition 7.1. *The automorphism group of some space X is the group consisting of automorphisms of X. In other words, it is the group consisting of transformations that map X back to itself.*

7.2.2 Flag Complex

Definition 7.2. *A flag complex is a simplicial complex X that is completely determined by its 1-skeleton. In other words, the maximal simplicial complex that the set of one-dimensional simplices outlines must be equivalent to X.*

Example 7.1. *In figure 7.1, simplicial complex A is not a flag complex, but simplicial complex B is. We see that the maximal simplex outlined by the 1-skeleton of A is note equivalent to A. If this were the case, A would contain two 2-simplicies instead of just one.*

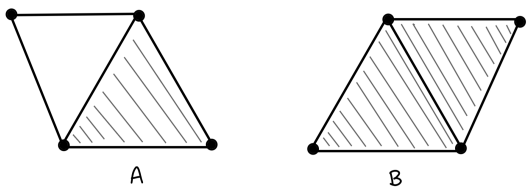

Figure 7.1 Simplicial complex B is a flag complex, while simplicial complex A is not.

It is known that $\Delta_{0,n}$ is a flag complex (Giansiracusa, 2016). Can we conclude the same thing about $\Delta^{(r,n)}$?

If $\Delta^{(r,n)}$ is a flag complex, this could help calculate its automorphism group, since the automorphism group of a flag complex is the same as the automorphism group of its one-skeleton.

Bibliography

Batyrev, Victor, and Mark Blume. 2009. On generalisations of losev-manin moduli spaces for classical root systems. *arXiv preprint arXiv:09122898* .

Brandt, Madeline. 2020. What is a moduli space? URL https://www.youtube.com/watch?v=aGbYg9d2KjQ.

Cavalieri, Renzo. 2016. Moduli spaces of pointed rational curves. *Lecture Notes for the Graduate Student School in the Combinatorial Algebraic Geometry program at the Fields Institute July* 18–22.

Chan, Melody. 2017. Lectures on tropical curves and their moduli spaces. *Moduli of Curves: CIMAT Guanajuato, Mexico 2016* 1–26.

Clader, Emily, Chiara Damiolini, Daoji Huang, Shiyue Li, and Rohini Ramadas. 2022. Permutohedral complexes and rational curves with cyclic action. *manuscripta mathematica* 1–52.

Deligne, Pierre, and David Mumford. 1969. The irreducibility of the space of curves of given genus. *Publications Mathématiques de l'IHES* 36:75–109.

Francisco, Christopher A, Jeffrey Mermin, and Jay Schweig. 2014. A survey of stanley–reisner theory. In *Connections between algebra, combinatorics, and geometry*, 209–234. Springer.

Giansiracusa, Noah. 2016. The dual complex of $\overline{M}_{0,n}$ via phylogenetics. *Archiv der Mathematik* 106:525–529.

Hassett, Brendan. 2003. Moduli spaces of weighted pointed stable curves. *Advances in Mathematics* 173(2):316–352.

Kock, Joachim, and Israel Vainsencher. 1999. Kontsevich's formula for rational plane curves. In *22nd Brazilian Mathematics Colloquium, Recife*.

Losev, Andrey, and Yuri Manin. 2000. New moduli spaces of pointed curves and pencils of flat connections. *Michigan Mathematical Journal* 48(1):443–472.

nLab authors. 2024. Euler characteristic. URL https://ncatlab.org/nlab/revision/Euler+characteristic/39.

Robinson, Alan, and Sarah Whitehouse. 1996. The tree representation of $\sum_{n+1}$. *Journal of Pure and Applied Algebra* 111(1-3):245–253.

Weisstein, Eric W. 2002. Stereographic projection. *Wolfram MathWorld* URL http://www. ams. org/publicoutreach/feature-column/fc-2014-02.